2018-06-01

Test Method for Predicting Failure Modes in Protective Films

Aubrey Jeanette Decker
Brigham Young University

Test Method for Predicting Failure Modes in Protective Films

Aubrey Jeanette Decker

A thesis submitted to the faculty of
Brigham Young University
in partial fulfillment of the requirements for the degree of

Master of Science

Andy R. George, Chair
Mike P. Miles
Barry M. Lunt

School of Technology

Brigham Young University

ABSTRACT

Test Method for Predicting Failure Modes
in Protective Films

Aubrey Jeanette Decker
School of Technology, BYU
Master of Science

In the business of packaging engineering, a large consumption of time is placed on evaluating new materials to provide cost savings to a company. This evaluation is made by using test methods such as those found in ASTM D4169-16, which helps to simulate shipping and distribution conditions. A key problem is that this test method can take up to multiple months, and sometimes years to complete. The apparatus created in this study allows for a comparison to be made between currently used films and prospective films in approximately ten hours. This allows for a prescreening of new films to be done before completing full ASTM shipment and distribution testing.

This study focuses on coextruded multilayer polymer films and the damage brought upon them in forms of puncture and abrasion through shipment and distribution.

Keywords: packaging, polymer films, predictive methods, shipping and distribution, abrasion, vibration, impact, puncture, thermoforming

ACKNOWLEDGEMENTS

I would like to express my gratitude for Dr. Andy George's great support during this process, and for continuing to let me pursue my passions. As well, I would like to thank Dr. Mike Miles and Dr. Barry Lunt for participating in my thesis committee and offering their guidance throughout this time. Additionally, a special thanks to Dr. Alan Boardman for this professional perspective in packaging technologies. I am also grateful for my sponsor for giving me the appropriate tools and expertise necessary for understanding and completing this project. Lastly, thank you to the Brigham Young University plastics and composites lab for providing me a space to work and for giving me help to complete my data collection for this research.

TABLE OF CONTENTS

LIST OF TABLES

LIST OF FIGURES

1 INTRODUCTION

1.1 Nature of the Problem

Packaging is an essential part of product development. It entails a thought-out system that protects products in transport, distribution, storage, purchasing, and end-use. To combat the effects that come from handling, many times multiple layers of protection are used to hold and distribute the product. These layers of packaging can be made from: corrugated or non-corrugated cardboard, hard or flexible polymer films.

Though any well-established company will most likely have films already being used to package their products, continuous improvement measures are often instigated to lower costs. Vendors have many different types of packaging films available that may be able to be purchased at a lower price, however they may not offer the same barrier and strength qualities that currently-used films provide. Each time a new type of film is proposed, it needs to be evaluated to make sure that it will provide the same or better properties that are found in the current film.

During packaging film evaluation, a series of tests are run on materials to ensure proper performance before being used on actual products for distribution. For this study, primary and secondary failure modes are abrasion and puncture respectively, and therefore the focus of this research will be on these two modes.

1.2 Purpose of This Research

Because of the amount of time it takes to prepare sample units and then run the test procedures, a need has been identified for a quicker test method to screen possible materials before running full standard tests on them. Currently the entire testing process can take months or even years, depending on a company's protocol and procedures. This testing consumes valuable resources both with employees, materials, and test equipment. And in many instances, results in no return on investment if the film does not comply with the necessary standards. In this research an apparatus and accompanying test method was developed to test unformed packaging films for the two specific modes of failure identified and their interactive affects. This system serves as a preliminary test method for new films before continuation with standard test procedures involving thermoformed package samples.

The focus of this research is on flexible films. To prove the system's effectiveness, a specific product line with its associated packaging materials was utilized. The assumption made was the methods created by this study can be modified and transferred to other products and their associated packaging, with the completion of this research.

1.2.1 Predicting Failure of Formed Materials Before They Are Formed

Due to the complex nature of multilayer, coextruded polymer films, the material composition of each film has a probability of effecting results. During the thermoforming process the film is heated and formed into the desired packaging geometry which results in various thicknesses across the package design features. When working with multiple layers, the forming temperature used for each layer also influences the final thicknesses and material properties of the final package. Six of the selected films, for example, contain polyamide as the

middle layer in varying percentages. The polyamide has a glass transition temperature on average of 132 °C, while the outer layers of the coextrusion on average have a glass transition temperature of 67 °C. As the outer layers have a glass transition temperature that is significantly lower than its inner layer, it would be expected that two outcomes are possible: the film's outer layers get over heated and burnt from trying to reach forming temperatures for the internal layers, or the internal layers do not reach forming temperatures and therefore are cold formed, creating excessive stress, or tearing in the film's inner layers during forming. For this reason, the properties before and after forming could be substantially different. A hypothesis of this study is that these differences between preformed and post-formed films is minimal enough, that pass-fail results in a durability test would agree between the two.

1.3 Research Objective

This research will provide a system used for predicting failure in post-formed films by comparing pre-formed films to current pre-formed films. Compared with the usual standardized qualification tests, this system will be able to decrease testing time for evaluating flexible films and reduce financial investment.

2 REVIEW OF THE LITERATURE

In studying the effects of distribution and handling of thermoformed packaging films the following information was gathered.

2.1 Thermoforming Behavior

Thermoformed products make up about five to six percent of polymers in the United States, and there are pros and cons to the process. The big advantage to thermoforming is its low cost. This low cost comes from the design of the process; significantly less pressure is needed for thermoforming in comparison to processes like injection molding, and tooling costs are lower seeing as the molds can be made from a variety of materials. This low mold cost also makes it relatively inexpensive for prototyping, with a relatively quick time frame from design to trial. Thermoformed parts are also economical to produce at low volumes for this reason. With thermoforming very thin products and very large products are also able to be made. Thermoforming can also be done with a variety of materials. For this reason, numerous physical and chemical properties can be given to the products being made, especially when multi-layer parts are made (ASTM F1929, 2015).

A large disadvantage of thermoforming comes with uneven wall thicknesses from the stretching of material on the mold. There are obvious disadvantages to this such as possible tearing of parts, or general lack of strength. Particularly when dealing with multilayer coextruded

films, uneven wall thickness can create layers which are too thin, therefore eliminating the properties that were planned in those stretched regions. Examples of these properties include, but are not limited to: oxygen and water permeability. Without the appropriate thickness, these areas may break or deform when faced with opposing forces (ASTM F1929, 2015) .

In a similar manner to the uneven wall thickness, thermoformed parts are stretched and pulled when they are forming against the mold, and on a deeper level, the chemical chains inside the thermoplastic sheet are being oriented. This may cause internal stresses inside the part, causing possible shrinkage and warping as the part ages, or gets exposed to heat, humidity, or sterilization. Such shrinkage and warping from these internal stresses often occur during validation testing of the thermoformed parts (ASTM F1929, 2015).

2.2 Multilayer Film Thermoforming Behavior

Thermoforming a single layer material is a complex science in understanding how different materials heat and stretch. This complexity is increased exponentially when using co-extruded multilayer polymers. The purpose of using these complex materials is to, hopefully, gain the material properties that each layer possesses as well as combat the less desirable properties (ASTM F1929, 2015).

As multilayer films exhibit these different advantages and disadvantages within each layer, different forming properties are also present. These differences could potentially lead to a variety of problems within the film after being formed. Cold forming occurs when a material is molded before reaching its optimum forming window. When this happens, different stresses are left in the chemical chains of the formed polymer, making it easier for warping or cracking to occur in the polymer as time and forces come into play (ASTM F2097, 2016). This premature forming

can also lead to the material changing in such a way that it is no longer clear, but instead, a hazy white (ASTM F1929, 2015). If a film has such compositions that the outer layers have a lower forming temperature window than the middle layers, cold forming can then occur in these middle layers. This cold forming could potentially cause internal stresses or may cause the inside layers to break apart instead of form to the mold geometry, possibly compromising the original purpose of the layer in certain regions of the formed part. While trying to adjust the temperatures to compensate for the internal temperatures needed, often the external layers can surpass their forming temperature window, causing stresses to appear, if not, causing melting, or even burning of these external layers (ASTM F2097, 2016).

2.3 Failure Modes Found in Current Packaging Films

As the varieties of packaging films have grown, more research has been done to investigate the advantages and disadvantages of the different compositions. Factors that are considered include (but are not limited to): cost, appearance, and protection against contamination and other common failure modes. Often facilities will allocate a considerable amount of time and resources for engineers to investigate the thinnest film (which generally comes at a lower cost) that will not be compromised during distribution and handling of the product. During shipping and distribution, vibration or repetitive rubbing allows the product to abrade against the film, which can lead to breakage of the barrier film. As would be expected, as the gauge of the film decreases, the probability of abrasion induced failures increases as there is less material to break through (ASTM F2097, 2016). Another common mode for failure in packaging films occurs when impact forces happen between the product and the film, leaving pinholes in the film. These pinholes, “allow unwanted communication between the product and the outside environment” (ASTM F1929, 2015). Whether it be through vibration or impact, these failures can be as small

as detracting from aesthetics to larger extremes such as making warning labels illegible or can even cause premature failure of the product (ASTM D996, 2016).

2.4 Current Methods for Simulating Shipment and Distribution

It would be ideal to eliminate all testing time but "it is extremely difficult to provide packaging engineers with fundamental information that can easily be applied. Often, the only answer is some form of physical testing" (ASTM F1929, 2015). Through years of research of impact and abrasion tests, compilations have been created to simulate the worst-case packaging distribution cycle. For instance, the Standard Practice for Performance Testing of Shipping Containers and Systems, "provides a uniform basis of evaluating, in a laboratory, the ability of shipping units to withstand the distribution environment (ASTM D4169, 2016). This is accomplished by subjecting them to a test plan consisting of a sequence of anticipated hazard elements encountered in various distribution cycles" (SPE Thermoforming, 2000).

To define the necessary forces, the size, weight, and form of the entire shipment unit is noted. This, along with consideration of the amount of anticipated damage during shipping and handling, the number of units to be shipped, and other criteria are all considered as the assurance level is established. On top of this, an acceptance criteria and distribution cycle are defined, and a test plan is written, all before testing is even started. Once testing is done, then results are evaluated and documented (SPE Thermoforming, 2000).

Because the primary sources of failure in interest to this study are abrasion and puncture, it was decided to place focus on the vibration test and the drop impact test (as individually outlined in ASTM D4169-16). Current standardized testing for the product line in interest to this study involves putting the shipping unit through a series of drops, then vibration, and then dropped

again. Each of these steps is defined further in their appropriate sections below (SPE Thermoforming, 2000).

2.4.1 Shipping Drop Test

To simulate manual handling of the package, a drop test is performed on the shipping unit. For units between 0-30 pounds, the drop height is 15 inches for the first round and the first 5 drops during the second round. The sixth drop in the second round is 30 inches (depending on the assurance level), with a decreasing drop height as weight increases (SPE Thermoforming, 2000) .

2.4.2 Shipping Vibration Test

Depending on the distribution cycle selected to try and replicate, a combination of truck, rail, and air profiles are selected for the duration of the vibration study being performed. In this combination, a spectrum of levels (g^2/Hz) are possible. Currently for distribution cycles 12 and 13, a 60-minute test is run on the truck profile, followed by a 120-minute test on the air profile. During this, to better simulate actual truck vibration environments, a combination of all three levels are recommended as depicted on the random Power Spectral Density Level Graph (which illustrates the levels of vibration force exhibited during shipment and distribution simulation). For this assessment, the specified product's shipment unit is placed directly on the vibration surface in the normal direction and the test is performed (SPE Thermoforming, 2000) .

2.5 Material Evaluation

To evaluate film integrity after the test procedure, multiple methods are available. One of the simplest of methods is the visual endpoint method, or in other words, just looking for a mark

or visual queue that the specimen has failed (Weinhold, 1997). Bubble emission testing is a common method involving a visual inspection for bubble streams coming from package defects – "all while it is submerged under water and gently pressurized". As defined by ASTM F2096, this system requires a closed system for air to be introduced (ASTM F2096, 2011). Another common method is to perform a Bell Jar test. In traditional Bell Jar tests, a sealed package is injected with dye, and then put under vacuum. By doing this, damage to the polymer materials can be seen as a result of migration of the dye from inside the package to outside the package (ASTM F1929, 2015; Tonrey, 1984).

2.6 Test Method Design

As with all test methods, many factors need to be considered to accurately represent the product and packaging behaviors that occur in real life situations. Test considerations for polymer testing include (Weinhold, 1997):

- Simulate the service conditions as closely as possible. A list of specifications for the service conditions must be compiled in advance.
- Be reproducible, yield quantitative results and be documentable.
- Yield results conducive directly or indirectly to improvements in material, product, and production.

By performing test methods this way, the study is more likely to produce information about what is expected for the integrity of the films.

2.6.1 Sample Quantity

Dr. Wayne Taylor (FDA recognized industry expert) concluded in a previous study for packaging durability testing, that one may decrease the sample quantity and still achieve a legitimate pass/fail results if the forces being applied are correspondingly increased, i.e. an inversely proportional relationship between force and sample quantity. This is due to the small number of failed samples which constitute a failure in packaging testing; the probability for a sample failure must be very low. Inducing that kind of failure can either be made with a high count of tested samples, or from increasing the forces to cause a higher probability for failure.

Particularly, in ASTM D4169-16, Taylor found that the stresses presented in the test are calculated to be five times greater than what a package will endure during its lifetime, therefore the acceptable sample size can be divided by five and still accurately represent what is necessary for real life situations [8]. By extension, this suggests that if a test's stress level is another five-fold higher than that of the ASTM conditions, the sample quantity can be further reduced to one fifth of the ASTM sample size and still achieve the same confidence in pass/fail results.

3 METHODOLOGY

It was expected that some modification and calibration would be necessary once the apparatus was built to account for the most significant departure of this test method from industry standards (ASTM): where the latter uses thermoformed films, and the former will use films before they are formed. These modifications would help make sure that the test accurately represents the forces being applied in ASTM testing while also inducing similar pass/fail test results. Unformed films of the baseline material were tested in this study's apparatus at the forces similar to ASTM testing, but no failures resulted from the test at these conditions. The greater thickness of the preformed films compared to the ASTM-tested thermoformed materials is assumed to account for ease at which the unformed samples passed the test with ASTM-like forces. A calibration test was performed, where the durations and forces were increased until failures were evident. These final forces were much higher than the original ASTM-mimicking forces but were required to reach the failure threshold of the thicker unformed films, thus allowing for better differentiation between the different candidate materials' durability. For this reason, a deviation description will be provided for each section to help explain the modifications from ASTM type testing.

3.1 Modifications to ASTM Methods

Through discussion with experts of the product line for this study, it was decided that the two most significant failure modes during package durability testing were abrasion and puncture. These can be directly correlated to the vibration and drop tests as defined by ASTM D4169-16. Further evaluation was completed to calculate the forces that occur on the packaging film materials during vibration and drop testing in ASTM, and how to represent those same forces in the simplified test in this study. In all cases, the worst-case forces from ASTM testing were targeted when designing the simplified test. Calculation of these forces is presented in the following sections.

3.1.1 Maximum Force in Impact

During standard drop testing the product corrugate shipper is dropped six times from a height of 15 inches in multiple orientations as per ASTM D4169-16. This is followed by the simulated distribution vibration test in accordance to ASTM D4169-16. Then a second round of drop tests involving five drops from a height of 15 inches (matching orientation patterns to the first round). Upon which a final drop in the single normal orientation from a height of 30 inches is performed.

The worst-case scenario during such testing is considered to be the 30-inch drop. Before calculating the impact force that occurs in this drop, the velocity of the shipper had to be defined. The final velocity before impact (v) was calculated in Equation 3-1, where g was gravity, and h was the height of the drop.

$$v = \sqrt{(2gh)} \tag{3-1}$$

The impact force (F) that occurs between the bottom of the shipment container and the ground during the 30" drop was calculated by substituting v from Equation 3-1 into Equation 3-2, where m was in the mass of the shipping unit, g was gravity, and s was the distance traveled after impact:

$$F = mg + \frac{m(v^2)}{2s} \tag{3-2}$$

The weight of the shipment container was measured to be five pounds, and 200 units were in each shipment container. It was necessary to calculate the distance s that the package compresses when it hits the ground after dropping from 30 inches, as this variable was unknown. By placing a ruler next to where the box would drop and recording 20 drops with a high-speed camera, the average compressive difference in height (representing the amount that would absorb into the ground) was measured to be approximately 0.118 inches. Using this distance, and Equations 3-1 and 3-2, the impact force was calculated and then divided by the number of individual packages in the shipment container (to find the average impact force per package) equaling 6.89 pounds per package.

3.1.2 Maximum Force in Vibration

ASTM D4169-16 has two separate vibration cycles that the packages go through, one that represents the vibration that occurs on a truck, and one for simulating air transport. These cycles can be seen in Figure 3-1 and Figure 3-2 respectively.

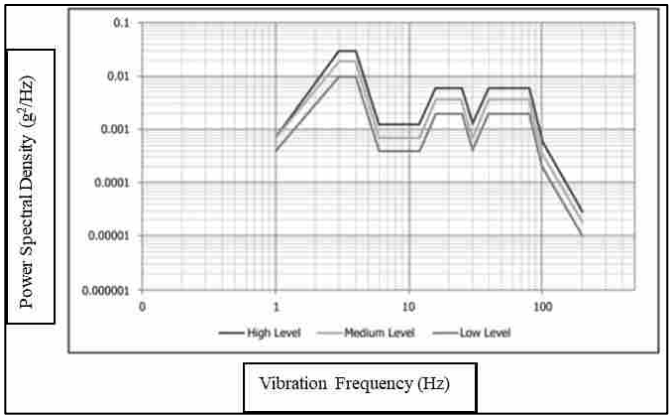

Figure 3-1: Truck Profile

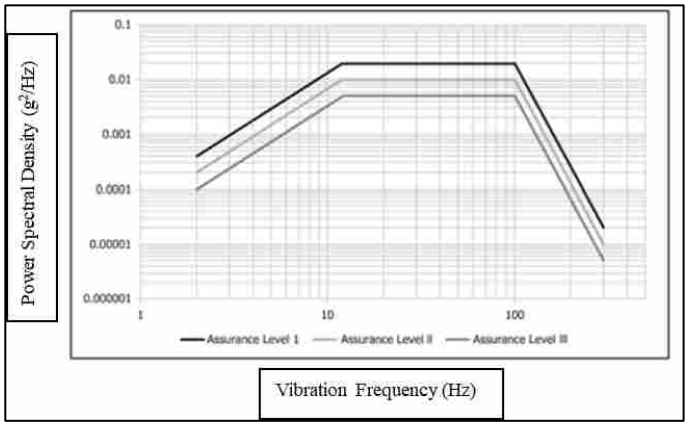

Figure 3-2: Air Profile

Of the two cycles, the truck variation was determined to be more aggressive in terms of g^2/Hz. The three lines in Figure 1 correlate with the package weight. The package weights most relevant to this study pertained to the "medium-level" line. Thus, to account for the worst-case scenario, the highest peak of medium-level cycle (Figure 3-1), 0.018 g^2/Hz was determined to be the desired vibration force for the simplified test apparatus to simulate.

The packages receiving the most aggressive abrasion forces during vibration testing would be the packages on the bottom-most layer of the shipper box as they are being pushed down by

the weight of the packages placed on top of them while going through the testing. Therefore, during vibration both the forces of the vibration itself, as well as the weight being placed on top of the product were accounted for. These forces can be seen in Figure 3-3.

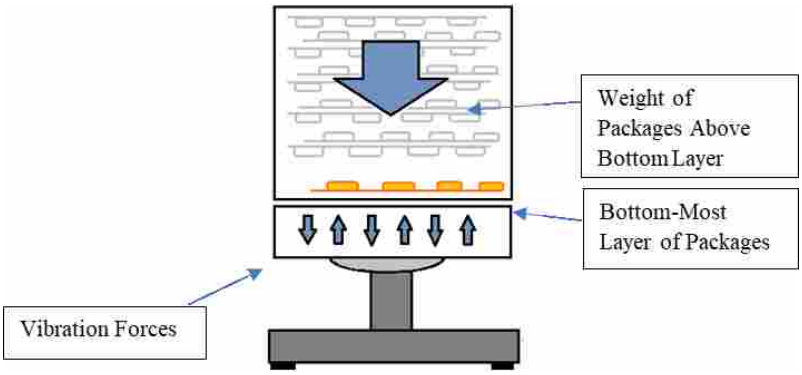

Figure 3-3: Forces During Vibration Testing

The film being used on the bottom layer of the package is interacting with the packaged product on one side, and then the carton, corrugate shipper box, and the vibratory table's metal platen on the other side (Figure 3-4).

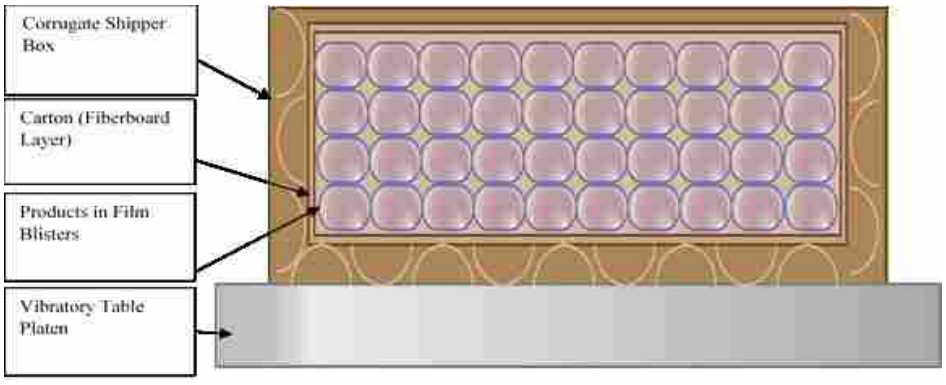

Figure 3-4: Cross Sectional Packaging Material Configurations

The vibration table that the package is placed on only moves in one direction, vertically. From the geometrical nature of the packages inside of the final package, it would be expected that while the device is being moved vertically during the vibration test, it would also shift horizontally. An evaluation was made by cutting a hole in the side of the shipment container (and the secondary carton) and attaching an accelerometer to an individual product on the bottom layer of the package. First, this was done by placing the accelerometer on the top of the individual package to track vertical movement, and then on the side to track horizontal movement. These observed motions are listed in Table 3-1 and the ratio between them was calculated.

Table 3-1: Directional Vibration Comparison

Accelerometer Configuration	Amplitude(Average)
Horizontal	0.10 mm
Vertical	0.97 mm
Amplitude Ratio (H/V)	0.10

3.1.3 Test Pattern

As mentioned, in current ASTM testing, the pattern for shipment and distribution testing is as follows: first drop sequence, both vibration sequences, second drop sequence. To simulate this pattern, the test apparatus would mimic the same forces in the following pattern: impact (puncture), vibration (abrasion), impact (puncture). Further justification for needing both modes of failure will be discussed in section 3.4 below.

3.1.4 Dye Penetration Leak Test for Defining Leaks in Samples

Figures 3-5 and 3-6 show example micrographs of the indentation damage from the impact tests. Both figures were taken at 5x magnification. In Figure 3-5 the indented portion of the material was measured to have an average diameter of 0.01 inches, while the pinhole had an average diameter of 0.008 inches. In figure 3-6, the indented portion was measured to have an average diameter of 0.012 inches. Therefore, a more robust test method was necessary as the pinholes found in samples were too small to be defined by visual inspection only.

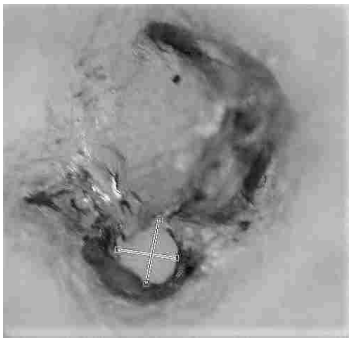

Figure 3-5: Kelpac (4mil) Leak

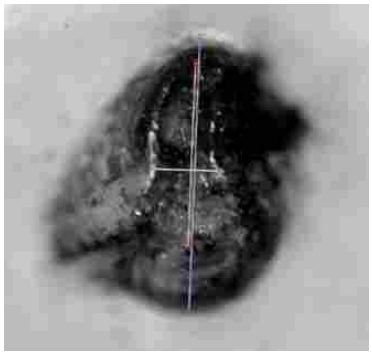

Figure 3-6: PE/PA (30%)/PE (5 mil) No Leak

As outlined by ASTM F1929-15, a specific formulation of blue dye can be made that is able to locate pinholes and seal leaks during packaging pouch post-test evaluation (ASTM F1929, 2015). Because the films being testing in this test method are not part of a sealed package, alterations were made to the current dye penetration test method. After the test sample went through the test apparatus cycle, it was placed on top of a generic paper towel (primarily used for soaking up excess dye; therefore, no specific brand/type is necessary), and a small polymer tip syringe was used to pull dye out of its container and put 0.1 mL on top of the sample where the suspect hole was. If the paper towel absorbed the blue dye, the test sample was defined as having a leak. If the paper towel stayed clean and the blue dye pooled on top of the sample, this sample was defined as not having a leak.

To further prove the necessity of this leak test, micrographs are presented in Figure 3-7 and Figure 3-8 to illustrate the difference between a sample with a leak, and a sample without a leak.

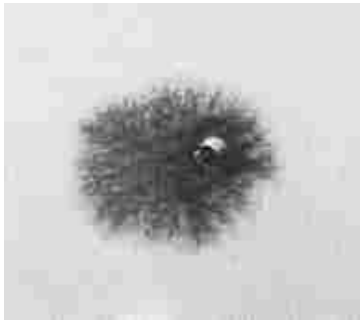

Figure 3-7: Dyed Sample with Pinhole Leak

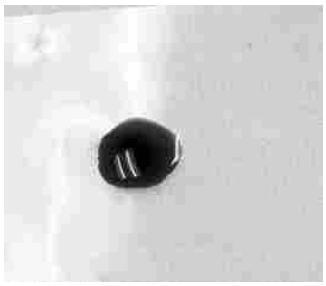

Figure 3-8: Dyed Sample with No Pinhole Leak

3.2 Materials

3.2.1 Selection of Previously Tested Films

Currently, the product is placed in a thermoformed blister consisting of one side of a bottom web, 8 mil K-Resin film. The 8 mil K-Resin is composed of ethylene-vinyl acetate (EVA), amorphous styrene (K-Resin), and then another layer of EVA. And a top web consisting of a polymer reinforced paper. The composition of the polymer reinforced paper is proprietary information per the paper pulp manufacturing company. Out of these two materials, more frequent failures are seen on the polymer film side of the package.

By evaluating the 8 mil K-Resin, a baseline was made for alternate films to be tested against. This baseline was created by evaluating 279 samples of K-Resin film to find the vibration duration required for leak failure of all samples in a 25-sample group, as well as a mean average vibration duration to leak failure, where all leak failures were confirmed in the dye leak test described in Section 3.1.4. While progressively trying different vibration durations, the duration was determined for such leak failure of all 25 samples in a group, and it was also determined that a slightly shorter duration resulted in no failures of a 25-sample group Other films could then be tested using the time-before-failure criteria, to see if the film candidates

perform better/adequately meeting the criteria, or worse than the currently used film by failing the criteria.

Previously tested materials, some that have failed and some that have passed at standard ASTM testing, were selected for this study. This allows a measure of validation of the simplified method, by comparing pass/fail results between ASTM results and the simplified test methodology in this study, i.e. a match in pass-fail results would suggest that the simplified test could be used as a pre-screening method to predict ASTM test results.

The films that have failed testing previously, their gauge thickness, and their compositions are listed in Table 3-2. Similar data for the films that have passed ASTM testing previously is listed in Table 3-3.

Table 3-2: Previously Failed Films

Material Manufacturer	Gauge	Film Composition
Bemis	4 mil	PE/PA (26%)/PE
Parnaplast	4 mil	PE/PA (20%)/PE
Kelpac	4 mil	Co-poly polyolefin (COC)
K-Resin	6 mil	EVA/K-Resin (amorphous styrene)/ EVA

Table 3-3: Previously Passed Films

Material Manufacturer	Gauge	Film Composition
Bemis	5 mil	PE/PA (30%)/PE
Bemis	5 mil	PE/PA (26%)/PE
Bemis	6 mil	PE/PA (26%)/PE
Bemis	4 mil	PE/PA (19%)/PE
Kelpac	6 mil	Co-poly polyolefin (COC)

3.2.2 Effects of Thermoforming

Through the nature of the thermoforming process the polymer film becomes thinner. For the mold and all candidate materials, the thinnest section of the film is approximately one third of the thickness of the preformed material. This was determined by measuring thickness differences (i.e. “gauge”) across the molded parts. The thinnest area of the post-formed film is expected to be the weakest point and most susceptible to leak failure in durability testing. The difference in thicknesses between the pre-formed films and the measured minimum thickness of the post-formed films was accounted for by increasing the forces applied until failure occurred in the baseline material at a similar rate to ASTM testing of the formed materials.

3.3 Test Apparatus Design

Figure 3-9 illustrates the test configuration designed and created for this study; the individual components are described hereafter.

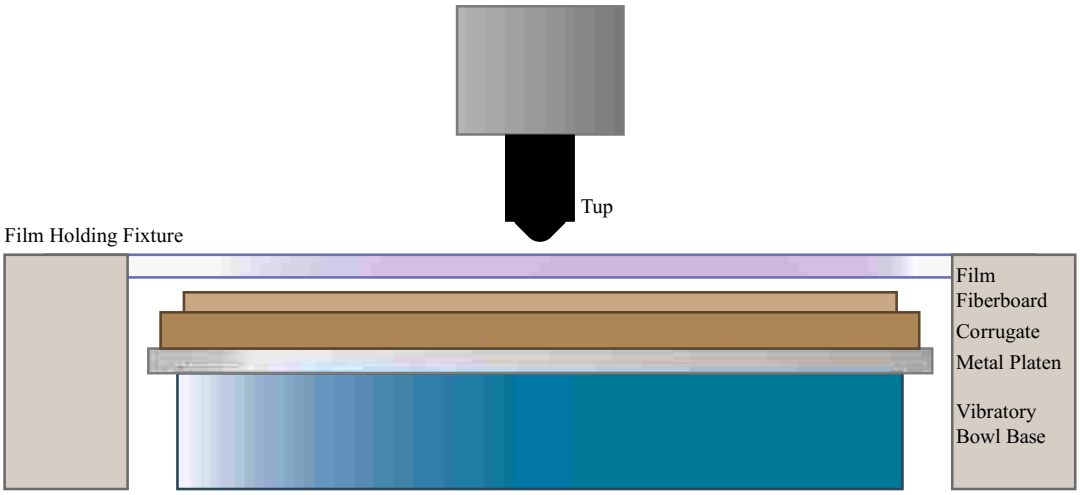

Figure 3-9: Configuration of Test Apparatus

3.3.1 Tup

While examining the current product packaging film failures that occur, the product geometry which most commonly causes failure was determined. To try and replicate this damage in the test apparatus, a 3D model was created of this product geometry. The harmful geometry serves as a tup for the puncture component of the test apparatus, thus simulating the puncture caused by the product inside the packaging. This was then 3D printed in a material that closely matched the characteristics found in that product. Currently, the product material is approved to be purchased from two vendors, so both vendor's polymer characteristics were considered. The desired properties to be matched were: tensile strength, modulus of elasticity, flexural strength, flexural modulus, and Rockwell hardness. These properties were comparable between the product material and the 3D printed material (See Table 3-4). Polymer tup materials proved to be somewhat problematic as they wore faster than a metal tip would have. But the trouble of inspecting and changing worn tips was warranted by the more accurate representation of the product hitting and rubbing against the film by matching surface friction and hardness.

Table 3-4: Tup Material Investigation

Property	Product Material 1	Product Material 2	3D Printed Material
Tensile Strength	50-65 MPa	n/a	63-65 MPa
Modulus of Elasticity	2000-3000 MPa	2400 MPa	2350 MPa
Flexural Strength	75-110 MPa	97 MPa	90 MPa
Flexural Modulus	2200 - 3200 MPa	2400 MPa	2300 MPa
Rockwell Hardness (M)	M73-77	M75	M70

Since this tup was made of a polymer, and was put under stress, mechanical damage was impossible to avoid. For this reason, before every test sample was run, a visual inspection was done to confirm that the tup geometry was not changed. This would mean no indentation, or bluntness to the tup tip. Regardless of the results of the visual inspection, the tup was changed after every fifth sample to prevent any imperfections that were missed during the inspection.

3.3.2 Tup Deviations

When originally selecting which tup geometry would be chosen for this study's impact testing, various packaged product geometries were considered. It was initially thought that the worst-case geometry (the most pointed) would cause leak failures too often in the film during the initial pneumatic strike. Therefore, to have a test method that would have some duration of time before failure, a less aggressive tup geometry was used, having a tup corner radius of 0.005". When a 3-D printed part is printed the resolution of the part is dependent on the filament used, and the first 3-D printed parts resulted in much larger corner radii. This was solved by setting the 3-D print geometry radius to 0" to allow for the actual radius to be equal to the desired radius at 0.005".

But this tup geometry proved to be too passive, causing only minor damage to the film, but not enough damage for a pinhole in the film to be made. As seen in Appendix A, Table A-1, multiple tests were run with this tup geometry, while also changing the pneumatic impact force, the number of strikes between the tup and the film, and the vibration force; these methods were not successful in producing a leak. For this reason, the tup geometry was evaluated again. The test geometry simulated an edge feature on the product. With further investigation of the current failure modes (puncture and abrasion) in commercial packaging products, the pinholes that were occurring were concluded to most likely occur on the corners of the design features, where the impact force in more concentrated in a smaller location on the packaging film. Understanding this, the tup model was tilted onto its side so that the corner feature would strike the film (Figure 3-10).

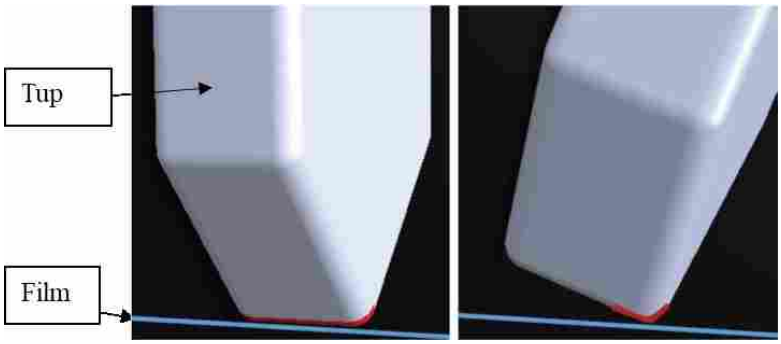

Figure 3-10: Tup Edge Orientation Vs. Tup Corner Orientation

Even then, with the corner-striking tup, the test was still not achieving the desired results necessary for creating pinhole failures in the film within the desired testing time. Therefore, the worst-case product tip geometry, was adopted after all, having a point-tip instead of a curvature radius.

3.3.3 Film Holding Fixture

The overall packaging configuration is comprised of multiple layers of materials and parts that all have interactions during the shipment process. These consist of the following: the product, the primary packaging materials (film), the secondary packaging materials (fiberboard), and the tertiary packaging materials (corrugated shipper box). During vibration as well as in drop tests although these entities are in a defined space with each other they exhibit minor independent motion and therefore cause interactive effects. For this reason, and for this study, replication of this interaction was determined to be necessary. The film was suspended between the secondary packaging and the tup (Figure 3-9). To do this, a frame fixture was made that extends around the vibratory bowl at the same height as where the fiberboard sits. The packaging film was then attached to the top of the arms of this frame to lay over the fiberboard, corrugate, and metal platen, while still maintaining movement freedom independent of the vibratory bowl's movement.

3.3.4 Film Holding Fixture Deviations

Before settling on the design seen above in Figure 3-9, the film holding fixture was placed directly on top of the vibratory bowl feeder base, where the bowl was originally placed. This was done by holding the film between two metal plates with a silicone O-ring separating the edges of the plates. These parts were tightened together using four thumb screws on each corner of the plate. On the top plate, a small portion was cut out to allow the tup to interact with the film. On the bottom plate, a hole was also cut so that the film, when indented by the tup, would not strike the metal plate. A model of this version can be seen in Figure 3-11.

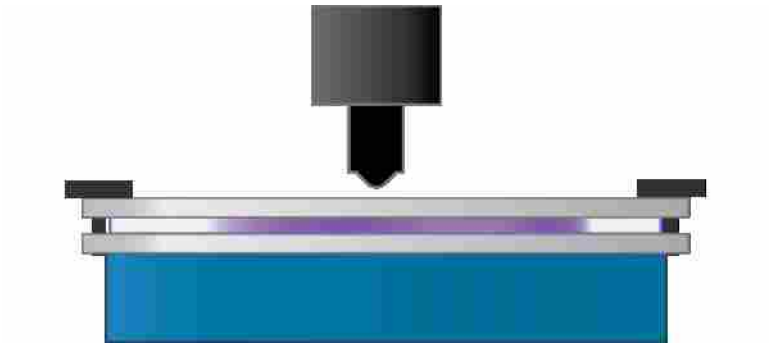

Figure 3-11: Initial Film Configuration

This model involved the film not having anything behind it while being tested. But this did not replicate the abrasion occurring in real life shipping and distribution, in which packages containing product rub against the interior natural fibers of the display carton. Therefore, it was important to support the test material as such. Corrugate materials as well as fiberboard were stacked underneath the film inside of the small hollow portion in the bottom plate of the holding fixture. This configuration can be seen in Figure 3-12.

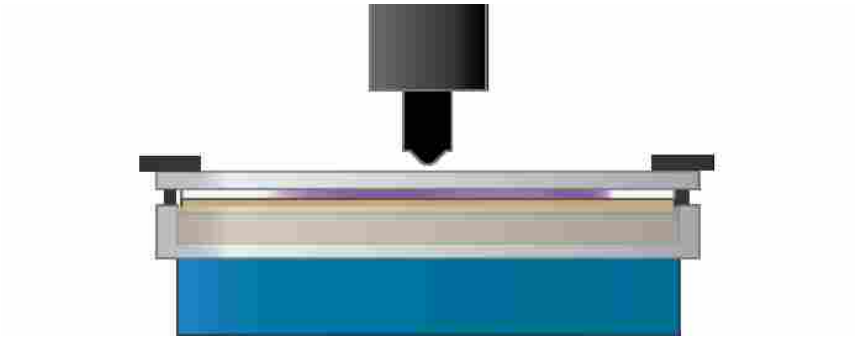

Figure 3-12: Film Holding Fixture with Packaging Material Support

Needing a more repeatable configuration, where the other packaging materials would stay consistent in thickness and position, the change was made to clamp down the corrugate and

fiberboard in the same silicon ring where the film was held (Figure 3-13). This made a marginal improvement in producing a more realistic representation of the ASTM D4169-16 test.

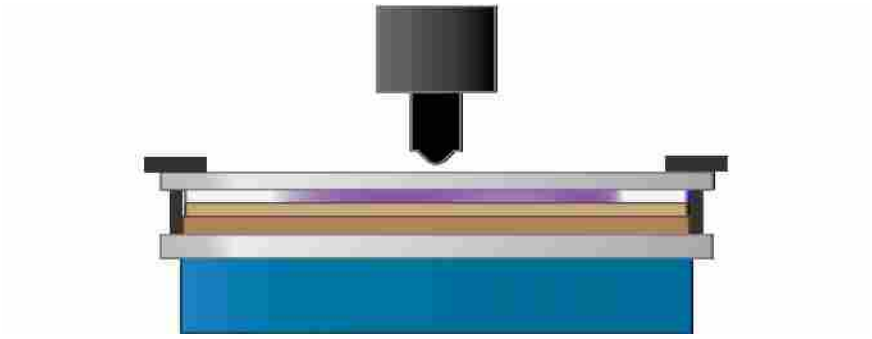

Figure 3-13: Film Holding Fixture with Clamped Packaging Materials

The apparatus was then re-designed to allow the film to move independently from the carton, as to create a more realistic representation of the real shipping and distribution modes. This allowed for the fibers of the carton to interact more with the film, causing damage as pressure was applied from the other side by the tup (mimicking the true product interaction inside of the packaging). The original holding fixture was replaced with a fixture that would be able to suspend the film away from the abrasive side, while still allowing for the contact to be made between the tup, the film, and the structure that both would have interactive motion.

An exterior frame was built that wrapped around the base of the vibratory bowl and sat at a height where the film would be held and suspended 0.015 to 0.05 inches away from the abrasive packaging materials on top of the vibratory bowl base. Seeing as the vibratory base was recorded to change in height by approximately 0.01 inches during vibration, this suggests that the film would not be in direct contact with the abrasive material (fiberboard) continually, but only when the tup forced the film to deflect downwards towards the fiberboard. The decided movement patterns are illustrated in Figure 3-14.

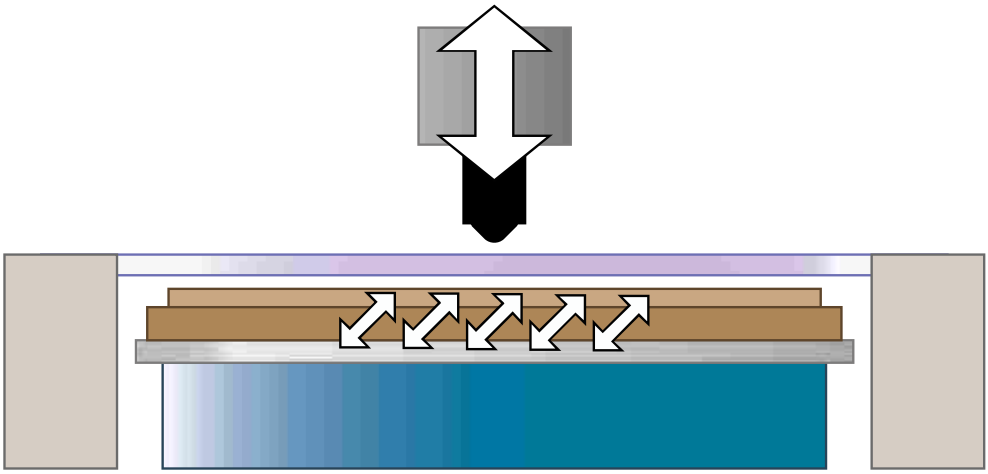

Figure 3-14: Directional Movement of Each Component

During the development of other tups, as well as the adjustment of the other variables, the abrasive backing was still altered in different configurations to make sure that the tup and film would have something to interact with but also making sure that this interaction was not too abrasive which would cause premature failures and less variability in the films integrity during the testing process. Testing with a solid aluminum plate, corrugate with the solid aluminum plate, fiberboard with the solid aluminum plate, or all three combined were tested. The most conclusive results came from the combination of the three materials, and this was validated by how well the pass/fail results mimicked the same results for each material in the previously performed ASTM testing. The data for these configurations can be found in Appendix A.

3.3.5 Impact Force Source

With a need for the impact force to be constant, reliable, and measurable, an actuator was chosen for replicating these forces. In determining the type of actuator to be used, the price, ease of use, and accuracy necessary were considered before choosing to use a pneumatic slide table.

By determining the impact force in the previous section, it was found that the chosen actuator could function at the same force when the regulator that would adjust the pneumatic input was set to 87 PSI (based upon a calculation of the pressure from the force and cross-sectional area of the impact surface).

3.3.6 Vibration Force Source

It was necessary to find a vibratory force that would both produce the necessary g^2/Hz value as well as provide an appropriate ratio between horizontal and vertical vibration, as was measured in section 3.1.2 (Table 3-1). A small vibratory bowl was tested to see if it could meet both requirements. First, the bowl was removed from the vibratory base so that the vibration could be passed through a flat base unit. An accelerometer was then placed on the vibratory base. Using LabView, the forces and frequencies were measured and then converted to g^2/Hz. A range controller was attached to the vibratory bowl which allowed an easy adjustment of the power supplied to the vibratory bowl. Table 3-5 lists the vibration forces measured at each range setting of the bowl controls. In order to achieve the same vibratory force on the vibratory bowl base to match the forces in the ASTM test, a force of 0.0182 g^2/Hz had to be produced through the vibratory bowl base. By adjusting the range dial on the vibratory bowl base between 3 and 4, the necessary force was found when the range setting was set to approximately 3.75. A marking was made on the range controller at this setting for reproducibility purposes in the test. Highlighted in Table 3-5 is the range setting on that range-controller necessary to replicate this force measured in the ASTM standard test (shown in Figure 3-1).

Table 3-5: g^2/Hz from Vibratory Bowl at Different Range Settings

Range	g^2/Hz
1	0.0041
2	0.0057
3	0.014
3.75	0.0182
4	0.0196
5	0.065
6	0.31
7	0.39
8	0.56
9	0.89
10	0.96

As mentioned in section 3.1.2, it was necessary to replicate the effects of vibration in both the vertical, as well as the horizontal plane. By reproducing this multidirectional behavior in the apparatus, a more accurate representation of vibratory effects could be made. To calculate the multidirectional behavior in the vibratory bowl base, the accelerometer was first placed on the side of the vibratory bowl base to measure the horizontal amplitude at each level on the range controller. Once this was measured, the accelerometer was placed on the top of the vibratory bowl base to measure the vertical amplitude at each level on the range controller. Identical to how the original relationship for the ASTM was determined, the average horizontal amplitude was divided by the average vertical amplitude to see the ratio between the horizontal and vertical forces in the vibratory bowl base. The comparison between the vibratory bowl and the ASTM standard vibration table are shown in Table 3-6. The measurements of ASTM standard vibration table are seen on the left side of the table, while the measurements of the vibratory bowl are shown on the right side of the table. In comparison, the amplitude ratio was equivalent for both tables, meaning they both operated the same proportionally in terms of horizontal versus vertical vibration.

Table 3-6: Horizontal vs. Vertical Vibration Amplitudes

Accelerometer Configuration	Amplitude (Average)
Horizontal	0.17 mm
Vertical	1.67 mm
Amplitude Ratio (H/V)	0.10

Accelerometer Configuration	Amplitude (Average)
Horizontal	0.10 mm
Vertical	0.97 mm
Amplitude Ratio (H/V)	0.10

Lastly, to replicate the weight that sits on top of the bottom-most layer of products in the shipping unit, a spring was placed between the tup and the actuator. While before, the tup could move vertically free in the unit, now the spring gave resistance equal to that of the weight of the products above the bottom-most layer. The weight was calculated using the Equation 3-3, where W_d was the weight being distributed onto a single product on the bottom most layer of the shipment container, W_a was the weight of all products in the shipment container, W_b was the weight of products in the bottom most layer of the shipment container and n_b was the number of products in the bottom most layer of the shipment container:

$$W_d = (W_a - W_b)/n_b \tag{3-3}$$

The spring force needed to replicate the weight being carried by one product on the bottom-most layer of the shipment container (F_w) was calculated using Equation 3-4, where k is the spring constant and x is the displacement of the spring during vibration.

$$F_w = kx \tag{3-4}$$

The displacement *x* was determined by evaluating the vertical distance that the vibratory bowl base traveled during use.

By making the latter half of each of these equations equal and then solving for *k*, the final equation was made for determining what spring should be used and can be seen below.

$$k = (\frac{W_a - W_b}{n_b})/x \quad (3\text{-}5)$$

3.3.7 Vibration Force Source Deviations

Originally, it was desired that the vibratory force produced by the vibratory bowl would be equal to that of the ASTM standard. When experimenting with this level no damage was found to the film. As mentioned, the thickness between the film before and after it was formed was thought to have a significant impact on the forces necessary for producing failure. For this reason, during testing, the range value was increased from 0.0182 g^2/Hz to 0.39 g^2/Hz but at this value, still no notable damage was observed. Eventually, it was decided to attempt testing at 0.96 g^2/Hz, fifty times the original target vibration force, and the maximum output of the vibratory bowl. When this was done, damage was finally seen in many of the samples.

3.3.8 Full Apparatus System

All the previously mentioned components were combined into one system as illustrated in Figure 3-15. The tup interacts with the film throughout the test while the impact and vibration components are programmed to work in sequence with one another.

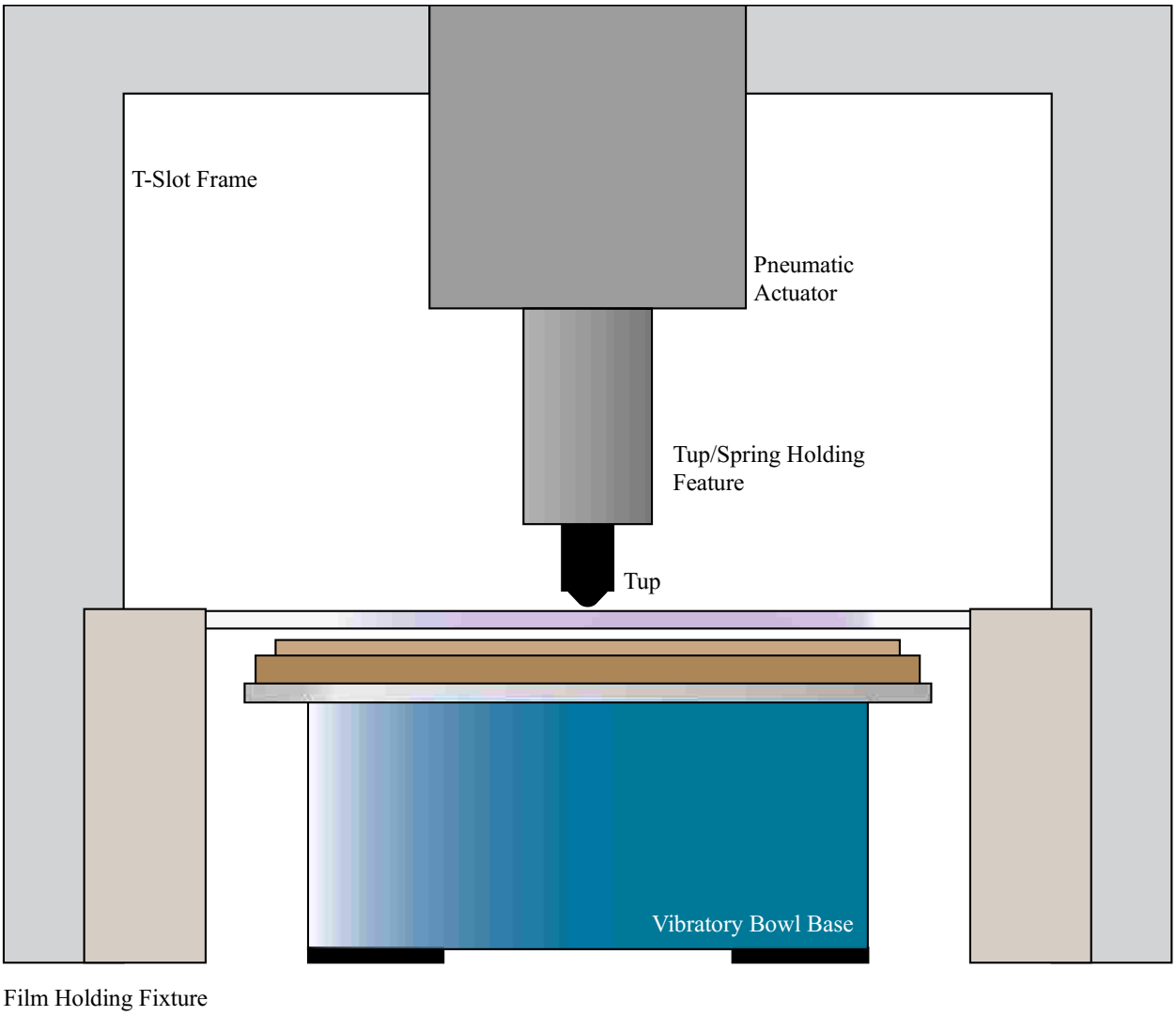

Figure 3-15: Full Apparatus Configuration

The tup was attached to the moving part of the pneumatic cylinder with the spring placed inside of the tup holding feature (Figure 3-16). These components were attached to an extruded t-slot frame with an adjustable table that allowed for the pneumatic cylinder (and its attached tup) to be moved up or down. This facilitated both alterations to the apparatus as well as film sample loading and unloading during testing.

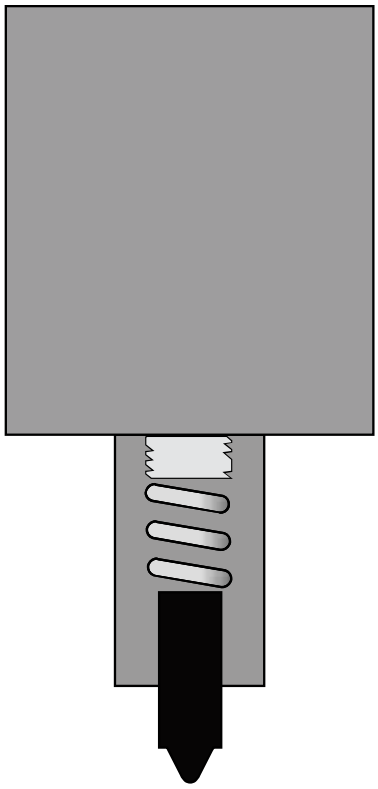

Figure 3-16: Spring/Pneumatic Configuration

The pneumatic actuator and the vibration table were connected to a human machine interface (HMI) and programmed with a programmable logic controller (PLC). In combination, the HMI module was programmed for the number of pneumatic strikes, duration of vibration, and number of secondary pneumatic strikes per the established baseline parameters set up.

3.3.9 Full Apparatus System Deviations

In original discussion, it was thought that the apparatus would be configured in an Instron tensile testing device. As this test focuses more on comparative pass/fail results, rather than absolute force numbers, it was not necessary to consistently monitor the forces being exhibited between the film and the tup. Thus, a customized aluminum frame was built to hold all the pieces in their necessary positions in lieu of an Instron test frame.

When developing the test method, and calculating values for the spring, it was thought that the tup should sit where it would just touch the film, without providing excess pressure during the vibration cycles; then during the impact cycles the small additional force of the spring could be disregarded in proportion to the force being given by the pneumatic cylinder. During testing, it was found that this pressure was not enough during the vibration cycles, therefore, alterations were made so that the pneumatic cylinder would be placed in such a position that the spring would be compressed during the testing, and only would decompress when the vibratory bowl base would move away from the tup as well as when the pneumatic cylinder would pull the tup away from the film before striking. This fix allowed for the final apparatus to work consistently as hoped for.

3.4 Baseline Establishment

Determination of the baseline consisted of determining the strike counts and vibration duration, and their corresponding forces where the current 8 mil K-resin film would always break (25 out of a group of 25 showing leaked samples). Initially the system baseline configuration was patterned following the ASTMD4169-16 standard to be the 15 pneumatic strikes, 2 hours of vibration, and 15 secondary pneumatic strikes. This baseline configuration did not produce any leak failures. Therefore, a series of design of experiments (DOE) were conducted to determine the test cycle required to cause the 25-for-25 failures, which was 23 strikes, then 60 minutes vibration, then 23 secondary strikes. Figure 3-17 and 3-18 below illustrate the process while changing these variables.

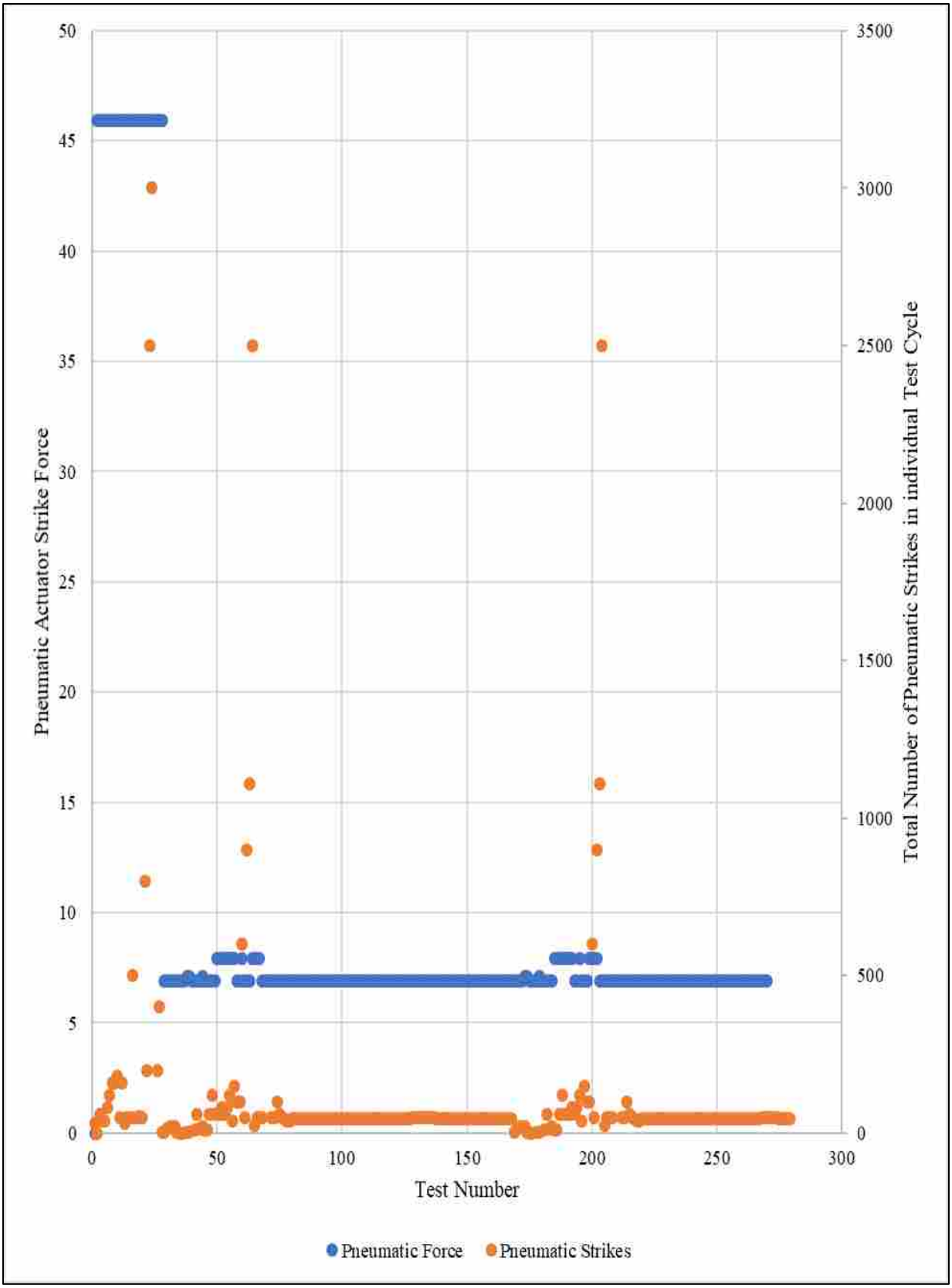

Figure 3-17: Baseline Development for Impact Variables

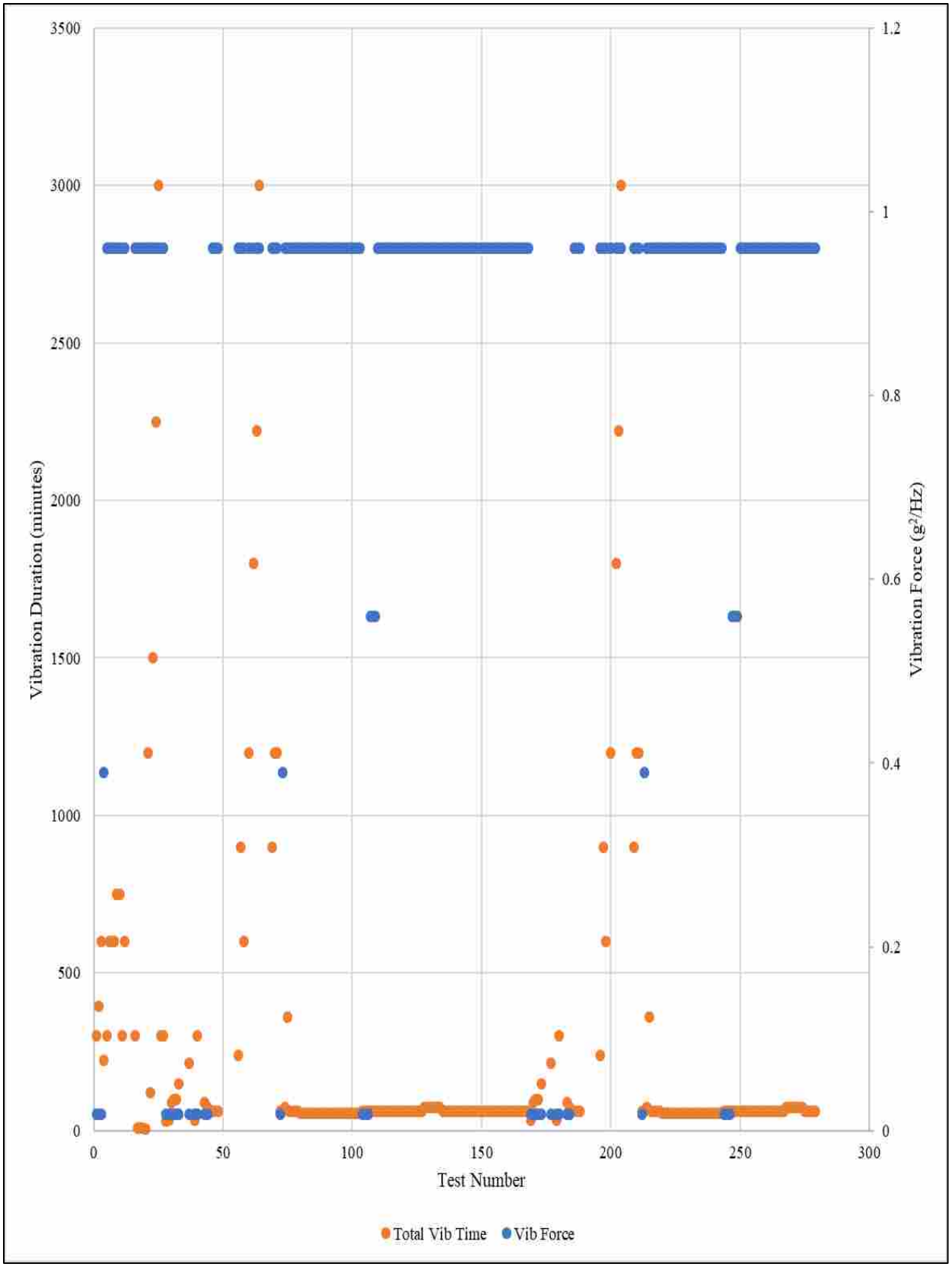

Figure 3-18: Baseline Development for Vibration Variables

The system test settings right below this total failure setting was then determined using similar methods. When diminishing the vibration duration from 60 minutes to 55 minutes (and keeping the strike counts the same), all 25 samples remained leak-proof. Thus, the target durability range for candidate materials was the entire cycle, with between 55 and 60 minutes in vibration. If a sample survived the cycle with 55 minutes of vibration, then it passed the minimum durability test. If a sample material failed with 60 minutes vibration duration, it does not mean an unsuitable material, rather only that it didn't perform better than the current material. As discussed in Section 3.2, if a film failed in previous ASTM testing, it would be expected to fail when being exposed to the test forces (vibration and impact). If a film passed previously in ASTM testing, it would be expected to pass this system with no leaks.

3.5 Apparatus Film Characterization

After the baseline test cycle was created, past tested films were selected as per Section 3.2, making sure to select films that had both failed and passed the ASTM testing. These films were then cut into eight 1.5"x11" samples with the 11-inch portion going in the machine direction of the film. This was seen not to effect films in initial testing whether cut in either direction as would be expected as the tup is striking in one location and the vibration cycles are vertical as well as rotational on the horizontal plane, i.e. no in-plane directionality of the test forces.

Typical ASTM sample count for packaging testing is 59 samples. As mentioned in Section 2.6.1, higher loads allow a smaller sample count. As the forces involved in this test were significantly higher than those in typical ASTM testing, a sample size of 10 was assumed to still provide adequate pass/fail confidence. This sample size was concluded per a conservative

approximation (approximately five times) of the stresses exhibited in ASTM over what normal packages would experience in real shipment and distribution conditions.

4 RESULTS

4.1 Apparatus Results

The nine material candidates (other than the baseline K Resin material) were tested on the apparatus following the established test cycle (23 pneumatic strikes with 6.89 pounds of force, 55-minute vibration duration at 0.96 g^2/Hz, and 23 more pneumatic strikes with 6.89 pounds of force) representing the minimum durability required for further consideration. Each material candidate was tested with a group of 10 samples. During this testing the following results were concluded.

Starting with the films that have previously failed shipping and distribution testing; the 4 mil Kelpac samples were found to have leaks in five out of the 10 samples. The K Resin 6 mil samples had eight with leaks, while one passing sample was completed with a dull tup. The 4 mil Parnaplast had only two leaks. Lastly, the 4 mil PE/PA (26%)/PE film had eight with leaks, though two of them are considered excusable by the fact that one test was done with a dull tup, and the other had a shift in the film from improper attachment of the film to its holding fixture. Results can be seen in Figure 4-1.

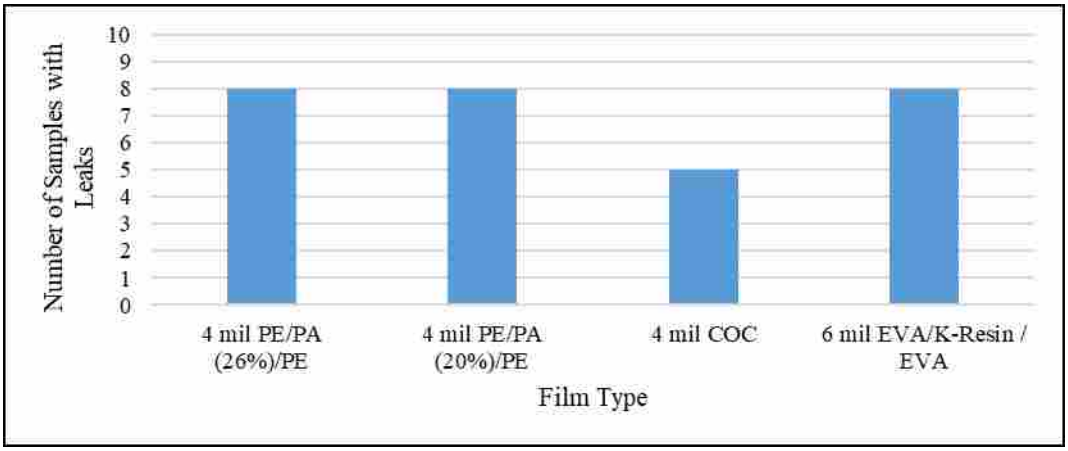

Figure 4-1: Leak Count for Films Which Previously Failed ASTM

As for the films that had previously passed shipping and distribution testing; 6 mil Kelpac and 4 mil PE/PA (19%)/PE both had no leaks in each 10-part sample group, which was predicted from their previous behavior in ASTM testing. 5 mil PE/PA (30%)/PE had two leaks, while 5 and 6 mil PE/PA (26%)/PE films each had three leaks per 10-part sample. Results can be seen in Figure 4-2.

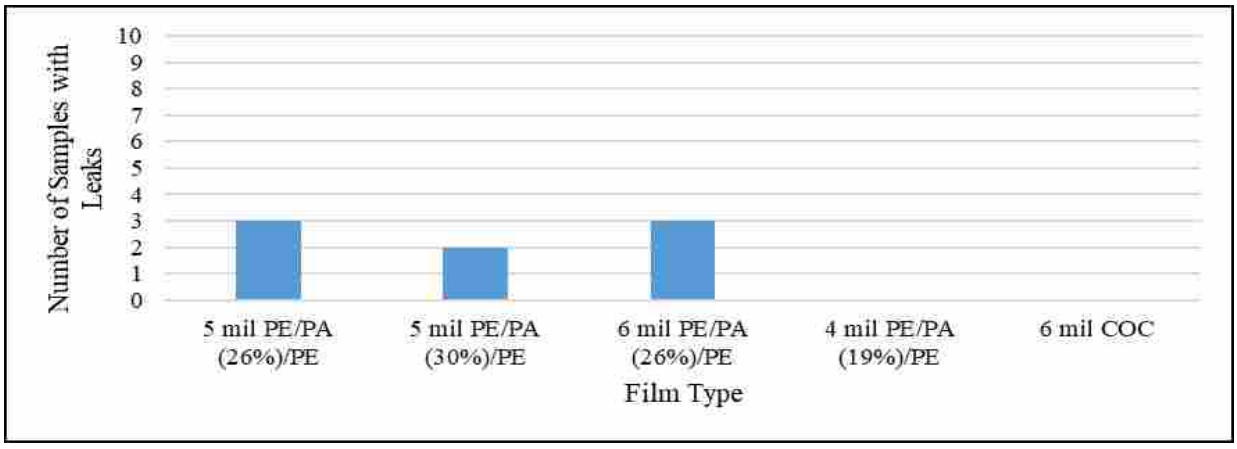

Figure 4-2: Leak Count for Films Which Previously Passed ASTM

4.2 Material Candidate Recommendations

During the ASTM standard shipment testing a film is considered failing if even one sample exhibits a leak or pinhole. Similarly, if this study's original hypothesis were correct, it would be expected that the films that had previously failed in ASTM testing would exhibit failure in at least one sample in the simplified test in this study. The films that had previously passed ASTM did indeed exhibit little to no leaks in this study's testing, and the films that had previously failed all exhibited at least one leak. This suggests that the apparatus is successful in being able to guide the user in screening materials before they are put through full ASTM shipment and distribution testing.

This test method is to be used as a prescreening evaluation to help the user determine if full ASTM testing should be executed. As this test relies on creating a baseline from an existing material (which passed ASTM testing) it could be that the baseline material's breaking point exceeds the forces that ASTM tests for farther than other films which may pass. Because of the complexity of thermoformed materials and their behaviors before and after being formed, it would be out of this scope to calculate the exact forces executed in ASTM and correlate them to translate to films before they are formed. For this scope, this test is considered adequate in guiding the user to know how a candidate film will behave in comparison to the current-used film.

The following three films had three or less leaks present after testing, because this proportion is low in comparison to the other candidate materials which previously failed, it would be up to the user to determine whether or not to proceed with testing. This could be determined by assessing cost, material properties, mold cavity geometry, etc.

- 5 mil PE/PA (30%)/PE
- 5 mil PE/PA (26%)/PE
- 6 mil PE/PA (26%)/PE

Meanwhile, two more materials (6 mil Kelpac and 4 mil PE/PA (19%)/PE) were found to exhibit no leaks at all, also suggesting their consideration as further candidate materials.

For further use of the apparatus, the user is able to determine whether or not they want to proceed with further ASTM study, but the following qualification would be suggested:

- Films with 0/10 samples containing leaks should proceed with ASTM testing
- Films with 4/10 or less samples containing leaks should be determined by the user on whether or not to proceed with ASTM testing
- Films with 5/10 or more samples containing leaks should not proceed with ASTM testing

4.3 Bimodal Failure

Additional testing was conducted, with either vibration or pneumatic strikes only (not in combination) (refer to Table 4-1 and Table 4-2). With up to 20 times the vibration duration and five times the number of pneumatic strikes (in comparison to the test cycle used above), both independent studies resulted in no pinholes.

It is reasonable to hypothesize that packaging film failure does not happen from impact or abrasion alone, but from a combination of the two. It is thought that the initial strikes from the pneumatic actuator allow the tup to begin breaking through the film, then the abrasion allows the microscopic chains inside the polymer to begin to shift and move to make way for the tup, then during the final pneumatic strikes the tup can easily break through the shifted polymer chains.

Table 4-1: Independent Vibration Test Samples

Test No.	g^2/Hz	Duration (minutes)
40	0.0182	300
69	0.96	900
70	0.96	1200
71	0.96	1200
177	0.0182	214
180	0.0182	300
209	0.96	900
210	0.96	1200
211	0.96	1200

Table 4-2: Independent Impact Test Samples

Test No.	Impact Force (lbs)	No. of Strikes
13	7.9	30
14	7.9	50
15	7.9	50
61	7.9	50
65	7.9	25
66	7.9	50
67	7.9	50
68	7.9	50
182	6.89	60
189	6.89	60
190	6.89	60
191	7.9	60
192	7.9	80
193	7.9	60
194	7.9	80
195	7.9	120
199	6.89	100
201	7.9	50
205	7.9	25
206	7.9	50
207	7.9	50
208	7.9	50

4.4 Polyamide Behavior

As many of the films selected contain a polyamide core structure, Figure 4-3 was compiled relating polyamide composition thickness with the number of leaks found during testing.

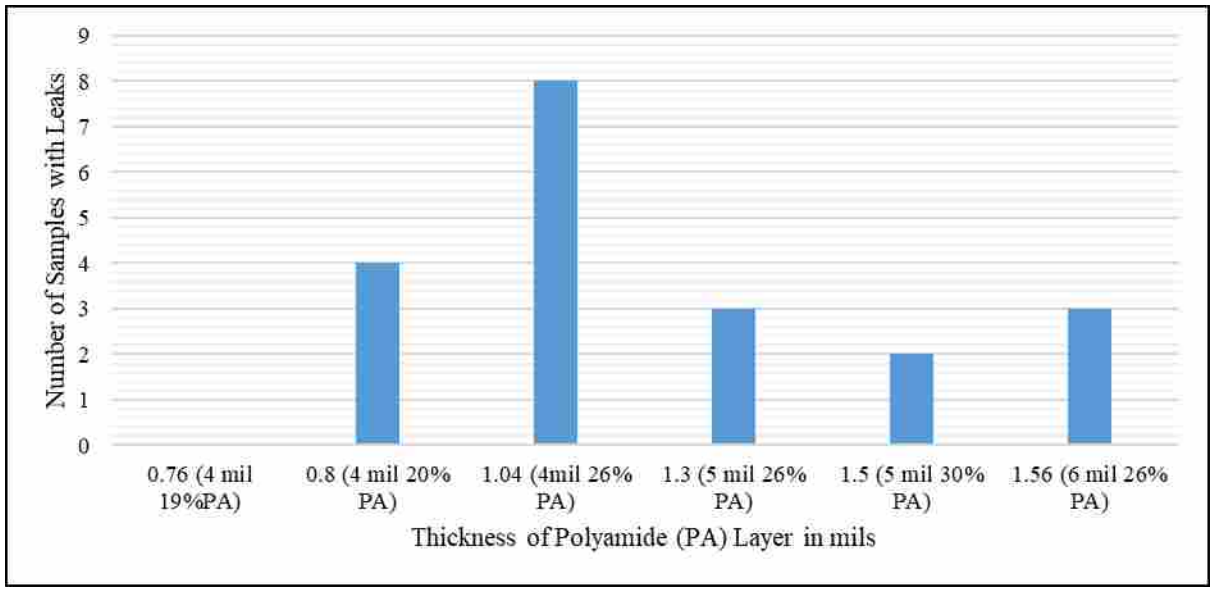

Figure 4-3: Polyamide Thickness vs. Leak Count

With this few of samples, it is hard to confirm that a relationship between the thickness of polyamide layers in every film type and the number of leaks in the 10 sample groups exists. It would be predicted that as the polyamide structure increased in thickness, the number of leaks would decrease. The major anomaly to this occurred in the PE/PA (19%)/PE, 4 mil sample set where no leaks were found in any of the films. Another unexpected result was the significant difference in failure between the 6 mil PE/PA (26%)/PE with 1.56 mil polyamide layer thickness and the PE/PA (30%)/PE with 1.5 mil polyamide layer thickness.

Table 4-3: Polyamide Failure by Film

Film Name	Thickness of Polyamide Layers	% of Failure
PE/PA (20%)/PE	0.8	80
PE/PA (19%)/PE	0.76	0
PE/PA (26%)/PE (4mil)	1.04	80
PE/PA (26%)/PE (5mil)	1.3	70
PE/PA (26%)/PE (6mil)	1.56	70
PE/PA (30%)/PE	1.5	20

Suspected reasons for these unexpected results are:

- The small sample size that these groups were tested in
- Variable tup sharpness and backing material

Because tup tips, and backing material were frequently replaced, it is more likely that these anomalies occur from the small sample size. PE/PA (26%)/PE films are defined by their percentage of polyamide (26%), three different versions of this polyamide composition ratio were used in this study, differing by their film thickness. When the PE/PA (26%)/PE with various thicknesses are looked at separately (see Figure 4-4) a negative exponential trend is rendered possible but would have to be investigated further with more than three points to confirm this trend. Another future recommendation is to extend the bracket for the PE/PA (26%)/PE film to include 3 and 8 mil samples, for further verification of the results trend.

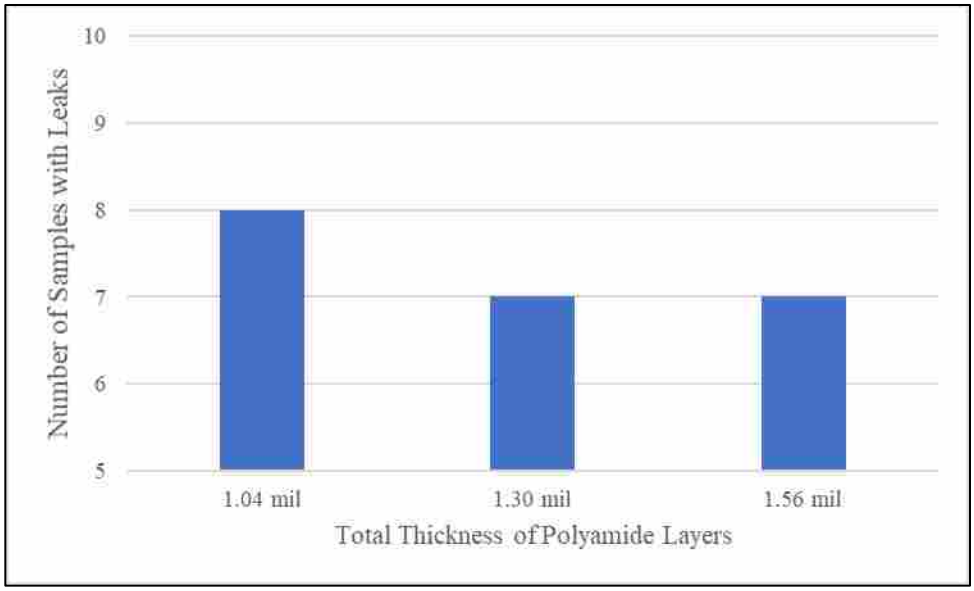

Figure 4-4: Sample Failure Count vs Polyamide Layer Thickness

4.4.1 Taber Test Correlation

A correlation study of formed materials versus non-formed materials was completed using a TABER Linear Abraser (TQC, 2018). The thickness of the Taber test samples from each material candidate were measured and recorded. The average thickness for each material was then plotted in Figures 4-5 through 4-8 against the average time-to-failure as measured in the Taber abrasion test, for the machine-direction (MD) and transverse-direction (TD) films as well as thermoformed samples. For the preformed films (Figures 4-5 and 4-6), the R^2 values for linear fits of the data were low enough to suggest that the small variances in thicknesses of these preformed films did not pose a significant relevance on the results in the test. While the low range in thickness in the preformed films caused little difference, the thermoformed samples (Figures 4-7 and 4-8) in contrast show a stronger and positive correlation between thickness and time-to-failure. This was intuitive, as the range in thickness inherent in a thermoformed part should be a strong prediction of how resistant the local area is to abrasion failure.

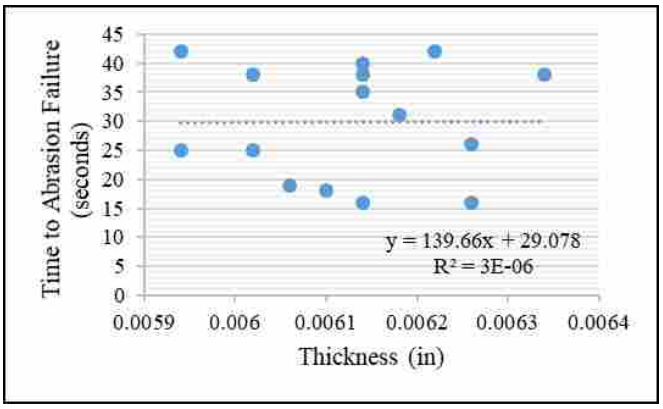

Figure 4-5: Preformed Material Abrasion Failure (MD)

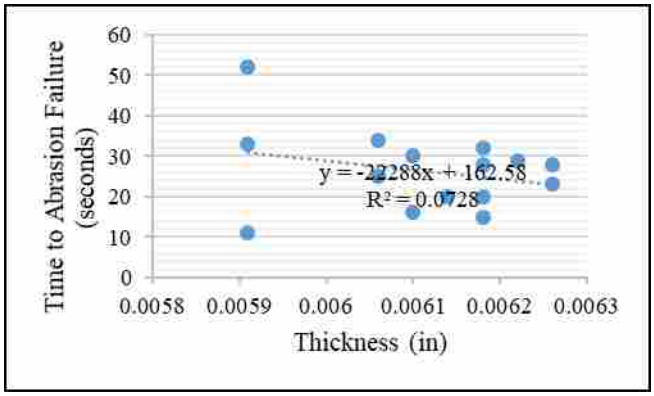

Figure 4-6: Preformed Material Abrasion Failure (TD)

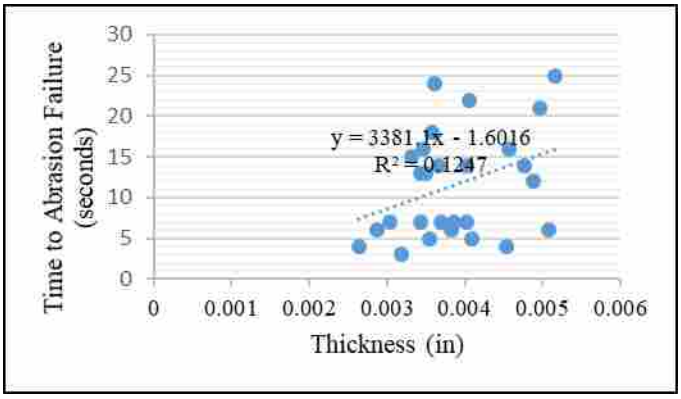

Figure 4-7: Formed Material Abrasion Failure (MD)

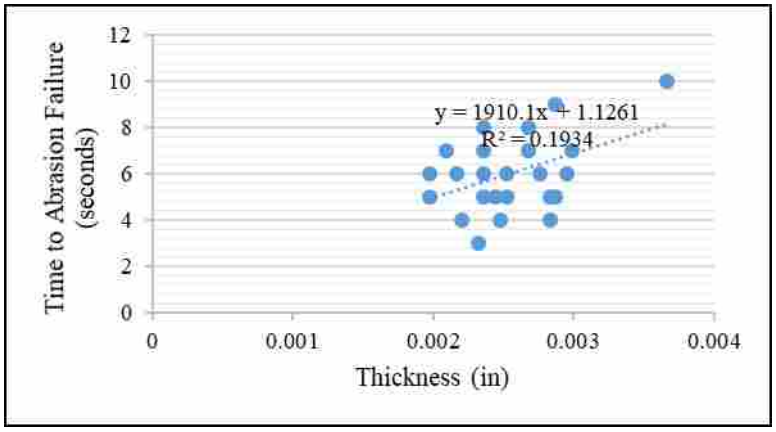

Figure 4-8: Formed Material Abrasion Failure (TD)

Sample data was organized and calculated to document each group's mean, minimum, lower quartile median, median, upper quartile median, and maximum time before abrasion failure (Table 4-4).

Table 4-4: Material Time to Failure Statistics

	Machine Direction		Transverse Direction	
	Unformed	Formed	Unformed	Formed
Mean	29.93	11.5185	24.57	5.826
Min	16	3	11	3
LQ	22	6	20	5
Med	31	12	28	6
UQ	38	16	31	7
Max	43	25	47.5	9

Calculations were also made to find and eliminate outliers by multiplying the interquartile range by 1.5 and finding samples outside of the normal range. These outliers were deleted from the sample set, but also examined in to see why they would have such unsuspected results. For ones lower than expected, often the probe in the abrasion tester was placed incorrectly on the sample, causing it to snag instead of abrading. For samples that resulted in higher than expected

values, the sample was often found to have types of particulate or oils on them, allowing the probe to glide more easily against the sample. These groups were then compared in terms of correlation between films before and after forming in the machine direction (Figure 4-9), and in the transverse direction (Figure 4-10). A linear regression was made for both sets of data with a good fit suggesting a strong prediction for formed sample Taber test results from unformed films in the same test. The slopes for each linear fit are less than one, signifying that the formed samples fail at shorter times than the unformed samples. This is most likely due to the localized thinning as well as forming weaknesses induced by thermoforming, resulting in a weaker material than the raw unformed films. The difference is greater for transverse direction samples.

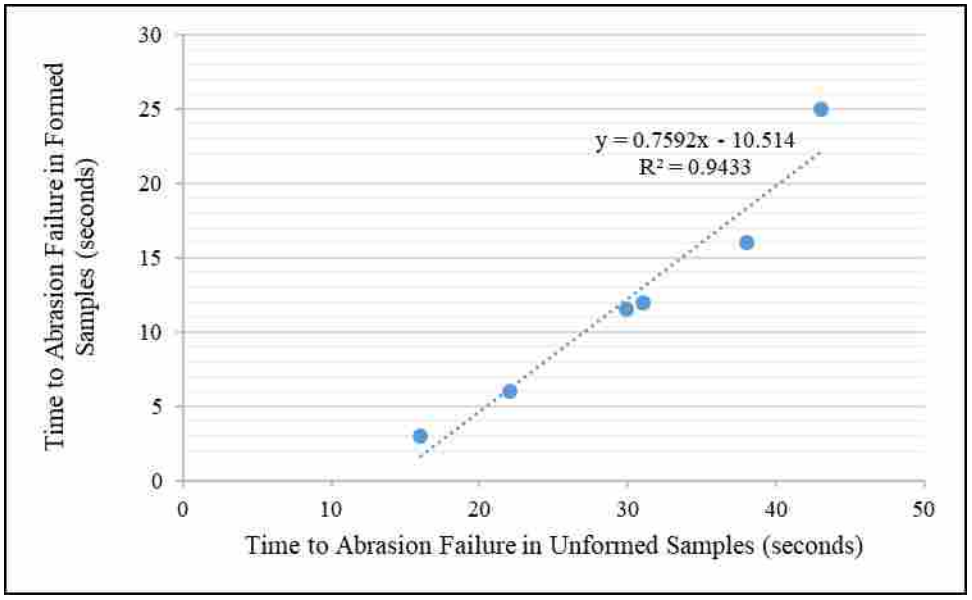

Figure 4-9: Linear Regression (MD)

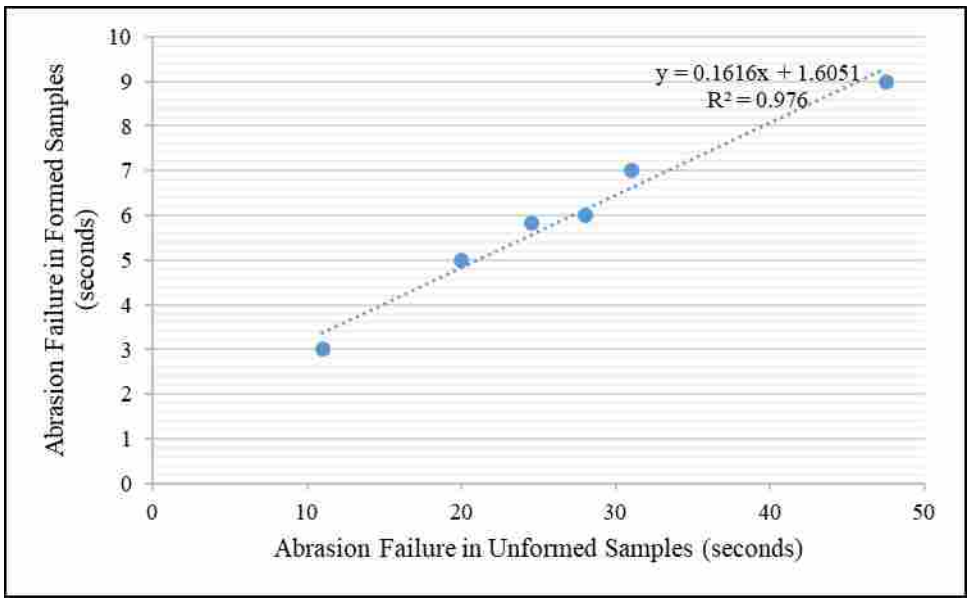

Figure 4-10: Linear Regression (TD)

In order to try and find an even higher R^2 value, exponential and logarithmic regressions were also considered. For samples in the machine direction, the following exponential function had a correlation of coefficeint of 0.9848 and an R^2 of 0.9698 (where U represents the unformed material time before abrasion failure and $f(U)$ represents the formed material time before abrasion failure):

$$f(U) = 1.0711(1.077^{U}) \tag{4-1}$$

Meanwhile, samples in the transverse direction followed a logarithmic regression with a correlation of coefficient of 0.98726 and an R^2 of 0.975, so the linear regression was seen as a better match. These results are presented in Table 4-5 and Figure 4-11, with functions from top to bottom in quadrant one: transverse direction, all samples together, and machine direction.

Table 4-5: Functions of Abrasion Failure Predictions Based on Orientations:

Abrasion Failure Relationship	Function	R^2
Machine Direction	$f(U)$ = 1.0711(1.077^U)	R^2= .9698
Transverse Direction	$f(U)$ = .1616U+1.6051	R^2= .976
All Samples Together	$f(U)$= 1.30748(1.07^U)	R^2= .974

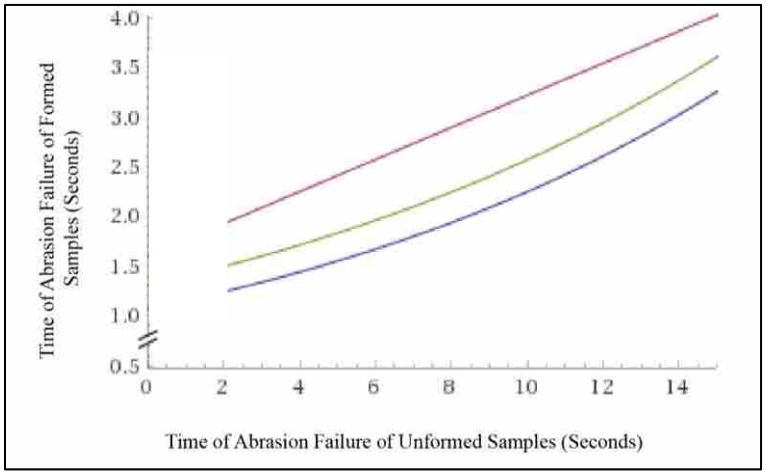

Figure 4-11: Regression for Each Group

By establishing this high of a R^2 between the unformed and formed samples and their times before abrasion failure, it was determined that the developed apparatus could potentially predict failure in the other materials being presented as well.

4.5 Future Recommendations

As was expressed previously, this system will work as a predictive method to help steer screenings of new films, to determine whether further investigation is advantageous. Future recommendations for making the device more accurate and efficient are as follows:

- Use a larger sample size when testing new materials to potentially create a more accurate representation of the post-form predictions.
- Extension of the sample in tension will change the mechanical properties due to polymer chain alignment. How sensitive the properties (e.g. durability in vibration or impact) are to this pre-tension are unknown, but it was assumed that such affects are small because of both the consistency in results as well as the low tension applied to the sample during loading. Further research should be done to investigate this importance and possibly incorporate a constant tension fixture to hold the sample.
- Incorporate multiple tups so that multiple tests can be done at once, therefore saving more test time.
- Find a way to automatically shut off the system when a leak is present.
    - Most likely this could be done by using a conductive polymer that is able to create an electric connection between the tup and the baseplate when the film breaks; like current abrasion test equipment.
- Automate the system so that film changes do not have to be done by the user, thus creating more efficient testing time.

5 SUMMARY OF STUDY

A test method was created that would assist in screening packaging film materials before putting them through full standard ship testing suite. By using a combination of impact force and vibration, an apparatus was created to take new film material candidates and compare them against the material that is currently being used for the product line being studied. In this study, materials that had previously failed shipment and distribution testing also failed in this test method (Figure 4-1), and materials that had previously passed shipment and distribution testing showed little to no failures in this test method (Figure 4-2). As this is a pre-screening process and not a defining test, judgement is expected to be made by the user as if to continue studying the proposed materials after being tested in the apparatus. This could be decided by material forming behavior, the shape of the mold, and where the geometries of the device will interact with the film after being formed. Furthermore, this test allows the user to compare prospective candidate materials to the material they are currently using in order to evaluate whether or not full standardized testing should be performed. By developing a pre-screening test that produces results in approximately 10 hours, this study can be considered successful. To replicate this for other products it would be necessary to reevaluate product geometries and create a unique baseline for the product and its corresponding film material. For greater user objectivity and more efficient testing, suggestions were made to increase the sample size and further automate the apparatus.

REFERENCES

ASTM Standard D4169-16, *Standard Practice for Performance Testing of Shipping Containers and Systems*. 2016, ASTM International.

ASTM Standard D996-16, *Standard Terminology of Packaging and Distribution Environments*. 2016, ASTM International

ASTM Standard F1929-15, *Standard Test Method for Detecting Seal Leaks in Porous Medical Packaging by Dye Penetration*. 2015, ASTM International.

ASTM Standard F2096-11*, Standard Test Method for Detecting Gross Leaks in Packaging by Internal Pressurization*. 2011: West Conshohocken, PA.

ASTM Standard F2097-16, *Standard Guide for Design and Evaluation of Primary Flexible Packaging for Medical Products*. 2016, ASTM International.

SPE Thermoforming, *The Forming Temperature.* Thermoforming 101, 2000. 19(2).
Taylor, W., *Reducing Sample Sizes and Stress Testing.* Guide To Acceptance Sampling 1992. 1.

Tonrey, J.F., *Non-Destructive Leak Testing of Blister and Strip Packaging for Pharmaceuticals.* Packaging technology Hillsdale, 1984. 14(2): p. 58-59.

TQC, https://www.tqc.eu/en/product/taber-linear-abraser-en/.

Weinhold, W.P., *Abrasion and scratch resistance of plastic parts.* Kunststoffe Plast Europe, 1997. 87(7): p. 23-24.

APPENDICES

APPENDIX A.

Table A-1: Data from 8 mil K-Resin Apparatus Calibration

Test No.	Probe	Pneumatic Strike Force (lbs)	Backing layers	Strike 1	Vib Level	Vib Time	Strike 2	Cycles	Results
1	Original Geometry	45.9	Air	3	3.75	60	3	5	No Leak
2	Original Geometry	45.9	Air	0	3.75	395	0	1	No Leak
3	Original Geometry	45.9	Air	3	3.75	60	3	10	No Leak
4	Original Geometry	45.9	Air	4	7	45	4	5	No Leak
5	Original Geometry	45.9	Air	4	10	60	4	5	No Leak
6	Original Geometry	45.9	Air	4	10	60	4	10	No Leak
7	Original Geometry	45.9	Air	6	10	60	6	10	No Leak
8	Original Geometry	45.9	Air	8	10	60	8	10	No Leak
9	Original Geometry	45.9	Air	8	10	75	8	10	No Leak
10	Original Geometry	45.9	Air	9	10	75	9	10	No Leak
11	Original Geometry	45.9	Carton+Corrugate	5	10	60	5	5	No Leak
12	Original Geometry	45.9	Carton+Corrugate	8	10	60	8	10	No Leak
13	Original Geometry	45.9	Carton+Corrugate	30	n/a	0	0	1	No Leak
14	Original Geometry	45.9	Carton+Corrugate	50	n/a	0	0	1	No Leak
15	Original Geometry	45.9	Corrugate (3)	50	n/a	0	0	1	No Leak
16	Original Geometry	45.9	Corrugate (3)	50	10	30	0	10	No Leak

17	Original Geometry	45.9	Corrugate (3)	0	10	10	50	1	No Leak
18	Original Geometry	45.9	Corrugate (3)	0	10	10	50	1	No Leak
19	Original Geometry	45.9	Corrugate (3)	2	10	10	50	1	No Leak
20	Original Geometry	45.9	Corrugate (3)	0	10	5	50	1	No Leak
21	Original Geometry	45.9	Corrugate (3)	20	10	60	20	20	No Leak
22	Original Geometry	45.9	Corrugate (3)	50	10	60	50	2	No Leak
23	Original Geometry	45.9	Corrugate (3)	50	10	60	50	25	No Leak
24	Original Geometry	45.9	Corrugate (3)	50	10	75	50	30	No Leak
25	Original Geometry	45.9	Corrugate (3)	60	10	75	60	40	No Leak
26	Less Radius Geometry	45.9	Corrugate (2)	10	10	30	10	10	No Leak
27	Less Radius Geometry	45.9	Corrugate (2)	20	10	30	20	10	No Leak
28	Less Radius Geometry	6.89	Air	2	3.75	30	2	1	No Leak
29	Less Radius Geometry	6.89	Air	2	3.75	30	2	1.1	No Leak
30	Less Radius Geometry	6.89	Air	2	3.75	30	2	3	No Leak
31	Less Radius Geometry	6.89	Air	2	3.75	20	2	5	No Leak
32	Less Radius Geometry	6.89	Air	2	3.75	20	2	5	No Leak
33	Less Radius Geometry	6.89	Air	2	3.75	30	2	5	No Leak
34	Less Radius Geometry	6.89	Air	2	n/a	0	0	1	No Leak
35	Less Radius Geometry	6.89	Metal Plate	1	n/a	0	0	1	No Leak
36	Less Radius Geometry	6.89	Metal Plate	1	n/a	0	0	1	No Leak
37	Less Radius Geometry	n/a	Air	0	3.75	214	0	1	No Leak
38	Less Radius Geometry	7.11	Air	4	n/a	0	0	1	No Leak
39	Less Radius Geometry	7.11	Corrugate (1)	2	3.75	30	2	1.1	No Leak
40	Less Radius Geometry	n/a	Air	0	3.75	300	0	1	No Leak

41	Less Radius Geometry	6.89	Air	10	n/a	0	0	1	No Leak
42	Less Radius Geometry	6.89	Air	60	n/a	0	0	1	No Leak
43	Less Radius Geometry	6.89	Corrugate (1)	2	3.75	25	2	3.52	No Leak
44	Less Radius Geometry	6.89	Corrugate (1)	2	3.75	15	2	5	No Leak
45	Less Radius Geometry	7.11	Corrugate (1)	10	n/a	0	0	1	No Leak
46	Less Radius Geometry	6.89	Air	5	10	60	5	1	No Leak
47	Less Radius Geometry	6.89	Air	30	10	60	30	1	No Leak
48	Less Radius Geometry	6.89	Air	60	10	60	60	1	No Leak
49	Less Radius Geometry	6.89	Air	60	n/a	0	0	1	No Leak
50	Less Radius Geometry	6.89	Air	60	n/a	0	0	1	No Leak
51	Less Radius Geometry	7.9	Metal Plate	60	n/a	0	0	1	No Leak
52	Less Radius Geometry	7.9	Metal Plate	80	n/a	0	0	1	No Leak
53	Less Radius Geometry	7.9	Carton+Corrugate	60	n/a	0	0	1	No Leak
54	Less Radius Geometry	7.9	Metal Plate+Carton+Corrugate	80	n/a	0	0	1	No Leak
55	Less Radius Geometry	7.9	Metal Plate+Carton+Corrugate	120	n/a	0	0	1	No Leak
56	Less Radius Geometry	7.9	Metal Plate+Carton	5	10	60	5	4	No Leak
57	Less Radius Geometry	7.9	Metal Plate+Carton	5	10	60	5	15	No Leak
58	Less Radius Geometry	7.9	Metal Plate+Carton	5	10	60	5	10	No Leak
59	Less Radius Geometry	6.89	Metal Plate	100	n/a	0	0	1	No Leak
60	Less Radius Geometry	6.89	Metal Plate+Carton+Corrugate	15	10	60	15	20	No Leak
61	Less Radius Geometry	7.9	Metal Plate+Carton	50	n/a	0	0	1	No Leak
62	Less Radius Geometry	6.89	Metal Plate+Carton	15	10	60	15	30	No Leak
63	Less Radius Geometry	6.89	Metal Plate+Carton	15	10	60	15	37	No Leak
64	Less Radius Geometry	6.89	Metal Plate+Carton	25	10	60	25	50	No Leak

65	Less Radius Geometry	7.9	Metal Plate+Carton+Corrugate	25	n/a	0	0	1	No Leak
66	Less Radius Geometry	7.9	Metal Plate+Carton+Corrugate	50	n/a	0	0	1	No Leak
67	Less Radius Geometry	7.9	Metal Plate+Carton+Corrugate	50	n/a	0	0	1	No Leak
68	Less Radius Geometry	7.9	Metal Plate+Carton+Corrugate	50	n/a	0	0	1	No Leak
69	Less Radius Geometry	n/a	Metal Plate+Carton+Corrugate	0	10	900	0	1	No Leak
70	Less Radius Geometry	n/a	Metal Plate+Carton+Corrugate	0	10	1200	0	1	No Leak
71	Less Radius Geometry	n/a	Metal Plate+Carton+Corrugate	0	10	1200	0	1	No Leak
72	Less Radius Geometry	6.89	Metal Plate+Carton+Corrugate	25	3.75	60	25	1	No Leak
73	Less Radius Geometry	6.89	Metal Plate+Carton+Corrugate	25	7.5	60	25	1	No Leak
74	Less Radius Geometry	6.89	Metal Plate+Carton+Corrugate	10	10	15	10	5	No Leak
75	Less Radius Geometry	6.89	Metal Plate+Carton+Corrugate	5	10	60	5	6	No Leak
76	Less Radius Geometry	6.89	Metal Plate+Carton+Corrugate	25	10	60	25	1	Leak
77	Less Radius Geometry	6.89	Metal Plate+Carton+Corrugate	23	10	60	23	1	Leak
78	Less Radius Geometry	6.89	Metal Plate+Carton+Corrugate	20	10	60	20	1	No Leak
79	Less Radius Geometry	6.89	Metal Plate+Carton+Corrugate	20	10	60	20	1	No Leak
80	Less Radius Geometry	6.89	Metal Plate+Carton+Corrugate	23	10	55	23	1	No Leak
81	Less Radius Geometry	6.89	Metal Plate+Carton+Corrugate	23	10	55	23	1	No Leak
82	Less Radius Geometry	6.89	Metal Plate+Carton+Corrugate	23	10	55	23	1	No Leak
83	Less Radius Geometry	6.89	Metal Plate+Carton+Corrugate	23	10	55	23	1	No Leak
84	Less Radius Geometry	6.89	Metal Plate+Carton+Corrugate	23	10	55	23	1	No Leak
85	Less Radius Geometry	6.89	Metal Plate+Carton+Corrugate	23	10	55	23	1	No Leak
86	Less Radius Geometry	6.89	Metal Plate+Carton+Corrugate	23	10	55	23	1	No Leak
87	Less Radius Geometry	6.89	Metal Plate+Carton+Corrugate	23	10	55	23	1	No Leak

88	Less Radius Geometry	6.89	Metal Plate+Carton+Corrugate	23	10	55	23	1	No Leak
89	Less Radius Geometry	6.89	Metal Plate+Carton+Corrugate	23	10	55	23	1	No Leak
90	Less Radius Geometry	6.89	Metal Plate+Carton+Corrugate	23	10	55	23	1	No Leak
91	Less Radius Geometry	6.89	Metal Plate+Carton+Corrugate	23	10	55	23	1	No Leak
92	Less Radius Geometry	6.89	Metal Plate+Carton+Corrugate	23	10	55	23	1	No Leak
93	Less Radius Geometry	6.89	Metal Plate+Carton+Corrugate	23	10	55	23	1	No Leak
94	Less Radius Geometry	6.89	Metal Plate+Carton+Corrugate	23	10	55	23	1	No Leak
95	Less Radius Geometry	6.89	Metal Plate+Carton+Corrugate	23	10	55	23	1	No Leak
96	Less Radius Geometry	6.89	Metal Plate+Carton+Corrugate	23	10	55	23	1	No Leak
97	Less Radius Geometry	6.89	Metal Plate+Carton+Corrugate	23	10	55	23	1	No Leak
98	Less Radius Geometry	6.89	Metal Plate+Carton+Corrugate	23	10	55	23	1	No Leak
99	Less Radius Geometry	6.89	Metal Plate+Carton+Corrugate	23	10	55	23	1	No Leak
100	Less Radius Geometry	6.89	Metal Plate+Carton+Corrugate	23	10	55	23	1	No Leak
101	Less Radius Geometry	6.89	Metal Plate+Carton+Corrugate	23	10	55	23	1	No Leak
102	Less Radius Geometry	6.89	Metal Plate+Carton+Corrugate	23	10	55	23	1	No Leak
103	Less Radius Geometry	6.89	Metal Plate+Carton+Corrugate	23	10	55	23	1	No Leak
104	Less Radius Geometry	6.89	Metal Plate+Carton+Corrugate	23	3.75	60	23	1	No Leak
105	Less Radius Geometry	6.89	Metal Plate+Carton+Corrugate	23	3.75	60	23	1	No Leak
106	Less Radius Geometry	6.89	Metal Plate+Carton+Corrugate	23	3.75	60	23	1	No Leak
107	Less Radius Geometry	6.89	Metal Plate+Carton+Corrugate	23	8	60	23	1	No Leak
108	Less Radius Geometry	6.89	Metal Plate+Carton+Corrugate	23	8	60	23	1	No Leak
109	Less Radius Geometry	6.89	Metal Plate+Carton+Corrugate	23	8	60	23	1	No Leak
110	Less Radius Geometry	6.89	Metal Plate+Carton+Corrugate	22	10	60	22	1	No Leak

111	Less Radius Geometry	6.89	Metal Plate+Carton+Corrugate	22	10	60	22	1	No Leak
112	Less Radius Geometry	6.89	Metal Plate+Carton+Corrugate	22	10	60	22	1	No Leak
113	Less Radius Geometry	6.89	Metal Plate+Carton+Corrugate	22	10	60	22	1	No Leak
114	Less Radius Geometry	6.89	Metal Plate+Carton+Corrugate	22	10	60	22	1	No Leak
115	Less Radius Geometry	6.89	Metal Plate+Carton+Corrugate	22	10	60	22	1	No Leak
116	Less Radius Geometry	6.89	Metal Plate+Carton+Corrugate	22	10	60	22	1	No Leak
117	Less Radius Geometry	6.89	Metal Plate+Carton+Corrugate	22	10	60	22	1	No Leak
118	Less Radius Geometry	6.89	Metal Plate+Carton+Corrugate	23	10	60	22	1	No Leak
119	Less Radius Geometry	6.89	Metal Plate+Carton+Corrugate	22	10	60	23	1	No Leak
120	Less Radius Geometry	6.89	Metal Plate+Carton+Corrugate	22	10	60	23	1	No Leak
121	Less Radius Geometry	6.89	Metal Plate+Carton+Corrugate	23	10	60	22	1	No Leak
122	Less Radius Geometry	6.89	Metal Plate+Carton+Corrugate	23	10	60	23	1	Leak
123	Less Radius Geometry	6.89	Metal Plate+Carton+Corrugate	23	10	60	23	1	Leak
124	Less Radius Geometry	6.89	Metal Plate+Carton+Corrugate	23	10	60	23	1	Leak
125	Less Radius Geometry	6.89	Metal Plate+Carton+Corrugate	23	10	60	23	1	Leak
126	Less Radius Geometry	6.89	Metal Plate+Carton+Corrugate	23	10	60	23	1	Leak
127	Less Radius Geometry	6.89	Metal Plate+Carton+Corrugate	23	10	60	23	1	Leak
128	Less Radius Geometry	6.89	Metal Plate+Carton+Corrugate	5	10	15	5	5	No Leak
129	Less Radius Geometry	6.89	Metal Plate+Carton+Corrugate	5	10	15	5	5	No Leak
130	Less Radius Geometry	6.89	Metal Plate+Carton+Corrugate	5	10	15	5	5	No Leak
131	Less Radius Geometry	6.89	Metal Plate+Carton+Corrugate	5	10	15	5	5	No Leak
132	Less Radius Geometry	6.89	Metal Plate+Carton+Corrugate	5	10	15	5	5	No Leak
133	Less Radius Geometry	6.89	Metal Plate+Carton+Corrugate	5	10	15	5	5	No Leak

134	Less Radius Geometry	6.89	Metal Plate+Carton+Corrugate	5	10	15	5	5	No Leak
135	Less Radius Geometry	6.89	Metal Plate+Carton+Corrugate	25	10	60	25	1	Leak
136	Less Radius Geometry	6.89	Metal Plate+Carton+Corrugate	25	10	60	25	1	Leak
137	Less Radius Geometry	6.89	Metal Plate+Carton+Corrugate	24	10	60	24	1	Leak
138	Less Radius Geometry	6.89	Metal Plate+Carton+Corrugate	24	10	60	23	1	Leak
139	Less Radius Geometry	6.89	Metal Plate+Carton+Corrugate	23	10	60	23	1	Leak
140	Less Radius Geometry	6.89	Metal Plate+Carton+Corrugate	23	10	60	23	1	Leak
141	Less Radius Geometry	6.89	Metal Plate+Carton+Corrugate	23	10	60	23	1	Leak
142	Less Radius Geometry	6.89	Metal Plate+Carton+Corrugate	23	10	60	23	1	Leak
143	Less Radius Geometry	6.89	Metal Plate+Carton+Corrugate	23	10	60	23	1	Leak
144	Less Radius Geometry	6.89	Metal Plate+Carton+Corrugate	23	10	60	23	1	Leak
145	Less Radius Geometry	6.89	Metal Plate+Carton+Corrugate	23	10	60	23	1	Leak
146	Less Radius Geometry	6.89	Metal Plate+Carton+Corrugate	23	10	60	23	1	Leak
147	Less Radius Geometry	6.89	Metal Plate+Carton+Corrugate	23	10	60	23	1	Leak
148	Less Radius Geometry	6.89	Metal Plate+Carton+Corrugate	23	10	60	23	1	Leak
149	Less Radius Geometry	6.89	Metal Plate+Carton+Corrugate	23	10	60	23	1	Leak
150	Less Radius Geometry	6.89	Metal Plate+Carton+Corrugate	23	10	60	23	1	Leak
151	Less Radius Geometry	6.89	Metal Plate+Carton+Corrugate	23	10	60	23	1	Leak
152	Less Radius Geometry	6.89	Metal Plate+Carton+Corrugate	23	10	60	23	1	Leak
153	Less Radius Geometry	6.89	Metal Plate+Carton+Corrugate	23	10	60	23	1	Leak
154	Less Radius Geometry	6.89	Metal Plate+Carton+Corrugate	23	10	60	23	1	Leak
155	Less Radius Geometry	6.89	Metal Plate+Carton+Corrugate	23	10	60	23	1	Leak
156	Less Radius Geometry	6.89	Metal Plate+Carton+Corrugate	23	10	60	23	1	Leak

157	Less Radius Geometry	6.89	Metal Plate+Carton+Corrugate	23	10	60	23	1	Leak
158	Less Radius Geometry	6.89	Metal Plate+Carton+Corrugate	23	10	60	23	1	Leak
159	Less Radius Geometry	6.89	Metal Plate+Carton+Corrugate	23	10	60	23	1	Leak
160	Less Radius Geometry	6.89	Metal Plate+Carton+Corrugate	23	10	60	23	1	Leak
161	Less Radius Geometry	6.89	Metal Plate+Carton+Corrugate	23	10	60	23	1	Leak
162	Less Radius Geometry	6.89	Metal Plate+Carton+Corrugate	23	10	60	23	1	Leak
163	Less Radius Geometry	6.89	Metal Plate+Carton+Corrugate	23	10	60	23	1	Leak
164	Less Radius Geometry	6.89	Metal Plate+Carton+Corrugate	23	10	60	23	1	Leak
165	Less Radius Geometry	6.89	Metal Plate+Carton+Corrugate	23	10	60	23	1	Leak
166	Less Radius Geometry	6.89	Metal Plate+Carton+Corrugate	23	10	60	23	1	Leak
167	Less Radius Geometry	6.89	Metal Plate+Carton+Corrugate	23	10	60	23	1	Leak
168	Less Radius Geometry	6.89	Metal Plate+Carton+Corrugate	23	10	60	23	1	Leak
169	Less Radius Geometry	6.89	Air	2	3.75	30	2	1.1	No Leak
170	Less Radius Geometry	6.89	Air	2	3.75	30	2	3	Leak
171	Less Radius Geometry	6.89	Air	2	3.75	20	2	5	Leak
172	Less Radius Geometry	6.89	Air	2	3.75	20	2	5	Leak
173	Less Radius Geometry	6.89	Air	2	3.75	30	2	5	Leak
174	Less Radius Geometry	6.89	Air	2	n/a	0	0	1	No Leak
175	Less Radius Geometry	6.89	Metal Plate	1	n/a	0	0	1	No Leak
176	Less Radius Geometry	6.89	Metal Plate	1	n/a	0	0	1	No Leak
177	Original Geometry	n/a	Air	0	3.75	214	0	1	No Leak
178	Less Radius Geometry	7.11	Air	4	n/a	0	0	1	No Leak
179	Less Radius Geometry	7.11	Corrugate (1)	2	3.75	30	2	1.1	No Leak

180	Less Radius Geometry	n/a	Air	0	3.75	300	0	1	No Leak
181	Less Radius Geometry	6.89	Air	10	n/a	0	0	1	No Leak
182	Less Radius Geometry	6.89	Air	60	n/a	0	0	1	No Leak
183	Less Radius Geometry	6.89	Corrugate (1)	2	3.75	25	2	3.52	No Leak
184	Less Radius Geometry	6.89	Corrugate (1)	2	3.75	15	2	5	No Leak
185	Less Radius Geometry	7.11	Corrugate (1)	10	n/a	0	0	1	No Leak
186	Less Radius Geometry	6.89	Air	5	10	60	5	1	No Leak
187	Less Radius Geometry	6.89	Air	30	10	60	30	1	No Leak
188	Less Radius Geometry	6.89	Air	60	10	60	60	1	No Leak
189	Less Radius Geometry	6.89	Air	60	n/a	0	0	1	No Leak
190	Less Radius Geometry	6.89	Air	60	n/a	0	0	1	No Leak
191	Less Radius Geometry	7.9	Metal Plate	60	n/a	0	0	1	No Leak
192	Less Radius Geometry	7.9	Metal Plate	80	n/a	0	0	1	No Leak
193	Less Radius Geometry	7.9	Carton+Corrugate	60	n/a	0	0	1	No Leak
194	Less Radius Geometry	7.9	Metal Plate+Carton+Corrugate	80	n/a	0	0	1	No Leak
195	Less Radius Geometry	7.9	Metal Plate+Carton+Corrugate	120	n/a	0	0	1	No Leak
196	Less Radius Geometry	7.9	Metal Plate+Carton	5	10	60	5	4	No Leak
197	Less Radius Geometry	7.9	Metal Plate+Carton	5	10	60	5	15	No Leak
198	Tilt Tip Probe	7.9	Metal Plate+Carton	5	10	60	5	10	No Leak
199	Tilt Tip Probe	6.89	Metal Plate	100	n/a	0	0	1	No Leak
200	Tilt Tip Probe	6.89	Metal Plate+Carton+Corrugate	15	10	60	15	20	No Leak
201	Tilt Tip Probe	7.9	Metal Plate+Carton	50	n/a	0	0	1	No Leak
202	Tilt Tip Probe	6.89	Metal Plate+Carton	15	10	60	15	30	No Leak
203	Tilt Tip Probe	6.89	Metal Plate+Carton	15	10	60	15	37	No Leak

204	Tilt Tip Probe	6.89	Metal Plate+Carton	25	10	60	25	50	No Leak
205	Point Tip Probe	7.9	Metal Plate+Carton+Corrugate	25	n/a	0	0	1	No Leak
206	Point Tip Probe	7.9	Metal Plate+Carton+Corrugate	50	n/a	0	0	1	No Leak
207	Point Tip Probe	7.9	Metal Plate+Carton+Corrugate	50	n/a	0	0	1	No Leak
208	Point Tip Probe	7.9	Metal Plate+Carton+Corrugate	50	n/a	0	0	1	No Leak
209	Point Tip Probe	n/a	Metal Plate+Carton+Corrugate	0	10	900	0	1	No Leak
210	Point Tip Probe	n/a	Metal Plate+Carton+Corrugate	0	10	1200	0	1	No Leak
211	Point Tip Probe	n/a	Metal Plate+Carton+Corrugate	0	10	1200	0	1	No Leak
212	Point Tip Probe	6.89	Metal Plate+Carton+Corrugate	25	3.75	60	25	1	No Leak
213	Point Tip Probe	6.89	Metal Plate+Carton+Corrugate	25	7.5	60	25	1	No Leak
214	Point Tip Probe	6.89	Metal Plate+Carton+Corrugate	10	10	15	10	5	No Leak
215	Point Tip Probe	6.89	Metal Plate+Carton+Corrugate	5	10	60	5	6	No Leak
216	Point Tip Probe	6.89	Metal Plate+Carton+Corrugate	25	10	60	25	1	Leak
217	Point Tip Probe	6.89	Metal Plate+Carton+Corrugate	23	10	60	23	1	Leak
218	Point Tip Probe	6.89	Metal Plate+Carton+Corrugate	20	10	60	20	1	No Leak
219	Point Tip Probe	6.89	Metal Plate+Carton+Corrugate	20	10	60	20	1	No Leak
220	Point Tip Probe	6.89	Metal Plate+Carton+Corrugate	23	10	55	23	1	No Leak
221	Point Tip Probe	6.89	Metal Plate+Carton+Corrugate	23	10	55	23	1	No Leak
222	Point Tip Probe	6.89	Metal Plate+Carton+Corrugate	23	10	55	23	1	No Leak
223	Point Tip Probe	6.89	Metal Plate+Carton+Corrugate	23	10	55	23	1	No Leak
224	Point Tip Probe	6.89	Metal Plate+Carton+Corrugate	23	10	55	23	1	No Leak
225	Point Tip Probe	6.89	Metal Plate+Carton+Corrugate	23	10	55	23	1	No Leak
226	Point Tip Probe	6.89	Metal Plate+Carton+Corrugate	23	10	55	23	1	No Leak

227	Point Tip Probe	6.89	Metal Plate+Carton+Corrugate	23	10	55	23	1	No Leak
228	Point Tip Probe	6.89	Metal Plate+Carton+Corrugate	23	10	55	23	1	No Leak
229	Point Tip Probe	6.89	Metal Plate+Carton+Corrugate	23	10	55	23	1	No Leak
230	Point Tip Probe	6.89	Metal Plate+Carton+Corrugate	23	10	55	23	1	No Leak
231	Point Tip Probe	6.89	Metal Plate+Carton+Corrugate	23	10	55	23	1	No Leak
232	Point Tip Probe	6.89	Metal Plate+Carton+Corrugate	23	10	55	23	1	No Leak
233	Point Tip Probe	6.89	Metal Plate+Carton+Corrugate	23	10	55	23	1	No Leak
234	Point Tip Probe	6.89	Metal Plate+Carton+Corrugate	23	10	55	23	1	No Leak
235	Point Tip Probe	6.89	Metal Plate+Carton+Corrugate	23	10	55	23	1	No Leak
236	Point Tip Probe	6.89	Metal Plate+Carton+Corrugate	23	10	55	23	1	No Leak
237	Point Tip Probe	6.89	Metal Plate+Carton+Corrugate	23	10	55	23	1	No Leak
238	Point Tip Probe	6.89	Metal Plate+Carton+Corrugate	23	10	55	23	1	No Leak
239	Point Tip Probe	6.89	Metal Plate+Carton+Corrugate	23	10	55	23	1	No Leak
240	Point Tip Probe	6.89	Metal Plate+Carton+Corrugate	23	10	55	23	1	No Leak
241	Point Tip Probe	6.89	Metal Plate+Carton+Corrugate	23	10	55	23	1	No Leak
242	Point Tip Probe	6.89	Metal Plate+Carton+Corrugate	23	10	55	23	1	No Leak
243	Point Tip Probe	6.89	Metal Plate+Carton+Corrugate	23	10	55	23	1	No Leak
244	Point Tip Probe	6.89	Metal Plate+Carton+Corrugate	23	3.75	60	23	1	No Leak
245	Point Tip Probe	6.89	Metal Plate+Carton+Corrugate	23	3.75	60	23	1	No Leak
246	Point Tip Probe	6.89	Metal Plate+Carton+Corrugate	23	3.75	60	23	1	No Leak
247	Point Tip Probe	6.89	Metal Plate+Carton+Corrugate	23	8	60	23	1	No Leak
248	Point Tip Probe	6.89	Metal Plate+Carton+Corrugate	23	8	60	23	1	No Leak
249	Point Tip Probe	6.89	Metal Plate+Carton+Corrugate	23	8	60	23	1	No Leak

250	Point Tip Probe	6.89	Metal Plate+Carton+Corrugate	22	10	60	22	1	No Leak
251	Point Tip Probe	6.89	Metal Plate+Carton+Corrugate	22	10	60	22	1	No Leak
252	Point Tip Probe	6.89	Metal Plate+Carton+Corrugate	22	10	60	22	1	No Leak
253	Point Tip Probe	6.89	Metal Plate+Carton+Corrugate	22	10	60	22	1	No Leak
254	Point Tip Probe	6.89	Metal Plate+Carton+Corrugate	22	10	60	22	1	No Leak
255	Point Tip Probe	6.89	Metal Plate+Carton+Corrugate	22	10	60	22	1	No Leak
256	Point Tip Probe	6.89	Metal Plate+Carton+Corrugate	22	10	60	22	1	No Leak
257	Point Tip Probe	6.89	Metal Plate+Carton+Corrugate	22	10	60	22	1	No Leak
258	Point Tip Probe	6.89	Metal Plate+Carton+Corrugate	23	10	60	22	1	No Leak
259	Point Tip Probe	6.89	Metal Plate+Carton+Corrugate	22	10	60	23	1	No Leak
260	Point Tip Probe	6.89	Metal Plate+Carton+Corrugate	22	10	60	23	1	No Leak
261	Point Tip Probe	6.89	Metal Plate+Carton+Corrugate	23	10	60	22	1	No Leak
262	Point Tip Probe	6.89	Metal Plate+Carton+Corrugate	23	10	60	23	1	Leak
263	Point Tip Probe	6.89	Metal Plate+Carton+Corrugate	23	10	60	23	1	Leak
264	Point Tip Probe	6.89	Metal Plate+Carton+Corrugate	23	10	60	23	1	Leak
265	Point Tip Probe	6.89	Metal Plate+Carton+Corrugate	23	10	60	23	1	Leak
266	Point Tip Probe	6.89	Metal Plate+Carton+Corrugate	23	10	60	23	1	Leak
267	Point Tip Probe	6.89	Metal Plate+Carton+Corrugate	23	10	60	23	1	Leak
268	Point Tip Probe	6.89	Metal Plate+Carton+Corrugate	5	10	15	5	5	No Leak
269	Point Tip Probe	6.89	Metal Plate+Carton+Corrugate	5	10	15	5	5	No Leak
270	Point Tip Probe	6.89	Metal Plate+Carton+Corrugate	5	10	15	5	5	No Leak
271	Point Tip Probe	6.89	Metal Plate+Carton+Corrugate	5	10	15	5	5	No Leak
272	Point Tip Probe	6.89	Metal Plate+Carton+Corrugate	5	10	15	5	5	No Leak

273	Point Tip Probe	6.89	Metal Plate+Carton+Corrugate	5	10	15	5	5	No Leak
274	Point Tip Probe	6.89	Metal Plate+Carton+Corrugate	5	10	15	5	5	No Leak
275	Point Tip Probe	6.89	Metal Plate+Carton+Corrugate	23	10	60	23	1	Leak
276	Point Tip Probe	6.89	Metal Plate+Carton+Corrugate	23	10	60	23	1	Leak
277	Point Tip Probe	6.89	Metal Plate+Carton+Corrugate	23	10	60	23	1	Leak
278	Point Tip Probe	6.89	Metal Plate+Carton+Corrugate	23	10	60	23	1	Leak
279	Point Tip Probe	6.89	Metal Plate+Carton+Corrugate	23	10	60	23	1	Leak

APPENDIX B.

Table B-1: Sample Results Tested for Comparison to Baseline

Film Type	Composition	Thickness (mils)	D4169 Pass/Fail	Results	Notes
Kelpac	COC	4	Fail	No Leak	
Kelpac	COC	4	Fail	Leak	
Kelpac	COC	4	Fail	No Leak	
Kelpac	COC	4	Fail	No Leak	
Kelpac	COC	4	Fail	No Leak	
Kelpac	COC	4	Fail	Leak	
Kelpac	COC	4	Fail	No Leak	
Kelpac	COC	4	Fail	Leak	
Kelpac	COC	4	Fail	Leak	
Kelpac	COC	4	Fail	Leak	
Kelpac	COC	6	Pass	No Leak	
Kelpac	COC	6	Pass	No Leak	
Kelpac	COC	6	Pass	No Leak	
Kelpac	COC	6	Pass	No Leak	
Kelpac	COC	6	Pass	No Leak	
Kelpac	COC	6	Pass	No Leak	
Kelpac	COC	6	Pass	No Leak	
Kelpac	COC	6	Pass	No Leak	
Kelpac	COC	6	Pass	No Leak	
Kelpac	COC	6	Pass	No Leak	
K- Resin	K Resin	6	Fail	No Leak	Dull Tup
K- Resin	K Resin	6	Fail	Leak	
K- Resin	K Resin	6	Fail	Leak	
K- Resin	K Resin	6	Fail	Leak	
K- Resin	K Resin	6	Fail	Leak	
K- Resin	K Resin	6	Fail	Leak	
K- Resin	K Resin	6	Fail	Leak	
K- Resin	K Resin	6	Fail	Leak	
K- Resin	K Resin	6	Fail	Leak	

K- Resin	K Resin	6	Fail	No Leak		
Parnaplast	20% Nylon	4	Fail	Leak		
Parnaplast	20% Nylon	4	Fail	Leak		
Parnaplast	20% Nylon	4	Fail	Leak		
Parnaplast	20% Nylon	4	Fail	Leak		
Parnaplast	20% Nylon	4	Fail	No Leak		
Parnaplast	20% Nylon	4	Fail	Leak		
Parnaplast	20% Nylon	4	Fail	Leak		
Parnaplast	20% Nylon	4	Fail	Leak		
Parnaplast	20% Nylon	4	Fail	Leak		
Parnaplast	20% Nylon	4	Fail	No Leak		
PE/PA (30%)/PE	30% Nylon	5	Pass	No Leak		
PE/PA (30%)/PE	30% Nylon	5	Pass	No Leak		
PE/PA (30%)/PE	30% Nylon	5	Pass	No Leak		
PE/PA (30%)/PE	30% Nylon	5	Pass	No Leak		
PE/PA (30%)/PE	30% Nylon	5	Pass	No Leak		
PE/PA (30%)/PE	30% Nylon	5	Pass	No Leak		
PE/PA (30%)/PE	30% Nylon	5	Pass	No Leak		
PE/PA (30%)/PE	30% Nylon	5	Pass	No Leak		
PE/PA (30%)/PE	30% Nylon	5	Pass	Leak		
PE/PA (30%)/PE	30% Nylon	5	Pass	Leak		
PE/PA (26%)/PE	26% Nylon	4	Fail	Leak		
PE/PA (26%)/PE	26% Nylon	4	Fail	No Leak	Dull Tup	
PE/PA (26%)/PE	26% Nylon	4	Fail	No Leak	Film shifted	
PE/PA (26%)/PE	26% Nylon	4	Fail	Leak		
PE/PA (26%)/PE	26% Nylon	4	Fail	Leak		
PE/PA (26%)/PE	26% Nylon	4	Fail	Leak		
PE/PA (26%)/PE	26% Nylon	4	Fail	Leak		

PE/PA (26%)/PE	26% Nylon	4	Fail	Leak
PE/PA (26%)/PE	26% Nylon	4	Fail	Leak
PE/PA (26%)/PE	26% Nylon	4	Fail	Leak
PE/PA (26%)/PE	26% Nylon	5	Pass	No Leak
PE/PA (26%)/PE	26% Nylon	5	Pass	No Leak
PE/PA (26%)/PE	26% Nylon	5	Pass	No Leak
PE/PA (26%)/PE	26% Nylon	5	Pass	No Leak
PE/PA (26%)/PE	26% Nylon	5	Pass	No Leak
PE/PA (26%)/PE	26% Nylon	5	Pass	Leak
PE/PA (26%)/PE	26% Nylon	5	Pass	No Leak
PE/PA (26%)/PE	26% Nylon	5	Pass	Leak
PE/PA (26%)/PE	26% Nylon	5	Pass	No Leak
PE/PA (26%)/PE	26% Nylon	5	Pass	Leak
PE/PA (26%)/PE	26% Nylon	6	Pass	No Leak
PE/PA (26%)/PE	26% Nylon	6	Pass	Leak
PE/PA (26%)/PE	26% Nylon	6	Pass	Leak
PE/PA (26%)/PE	26% Nylon	6	Pass	No Leak
PE/PA (26%)/PE	26% Nylon	6	Pass	No Leak
PE/PA (26%)/PE	26% Nylon	6	Pass	Leak
PE/PA (26%)/PE	26% Nylon	6	Pass	No Leak
PE/PA (26%)/PE	26% Nylon	6	Pass	No Leak
PE/PA (26%)/PE	26% Nylon	6	Pass	No Leak
PE/PA (26%)/PE	26% Nylon	6	Pass	No Leak

PE/PA (19%)/PE	19% Nylon	4	Pass	No Leak	
PE/PA (19%)/PE	19% Nylon	4	Pass	No Leak	
PE/PA (19%)/PE	19% Nylon	4	Pass	No Leak	
PE/PA (19%)/PE	19% Nylon	4	Pass	No Leak	
PE/PA (19%)/PE	19% Nylon	4	Pass	No Leak	
PE/PA (19%)/PE	19% Nylon	4	Pass	No Leak	
PE/PA (19%)/PE	19% Nylon	4	Pass	No Leak	
PE/PA (19%)/PE	19% Nylon	4	Pass	No Leak	
PE/PA (19%)/PE	19% Nylon	4	Pass	No Leak	
PE/PA (19%)/PE	19% Nylon	4	Pass	No Leak	